Original Article

Histological Study on the Effect of Rivastigmine and Coconut Oil on the Hippocampus of Experimentally Induced Alzheimer's Disease in Adult Male Albino Rats

Zeinab Mohamed Kamel Ismail, Mary Attia Morcos, Mennatallah Mohamed Ragai and Sarah Mohammed Alghandour

Department of Histology, Faculty of Medicine, Cairo University, Cairo, Egypt

ABSTRACT

Introduction and Objectives: Alzheimer's disease (AD) is a neurodegenerative disorder that represents the highest form of dementia. The hippocampus is one of the earliest areas affected in AD. Currently, there is no definitive cure for AD. This study was planned to evaluate the effect of rivastigmine and coconut oil (CO), alone or together, on aluminum chloride ($AlCl_3$)-induced AD model in the hippocampus of adult male albino rats.

Materials and Methods: Thirty three rats were divided into group I (control) and group II (experimental, subdivided into IIa, IIb, IIc, IId and IIe subgroups). AD was induced in group II by $AlCl_3$ for 45 days. Subgroup IIa was sacrificed at the 45th day, subgroup IIb was left without treatment for 30 days and subgroup IIc received rivastigmine for 30 days. Subgroup IId administered CO simultaneously with $AlCl_3$ then CO treatment continued for 30 days. Subgroup IIe administered CO simultaneously with $AlCl_3$ then CO treatment continued simultaneously with rivastigmine for 30 days. Y-maze memory test was performed and serum acetylcholinesterase (Ach-E) level was measured. After sacrifice, Ach-E and glutathione (GSH) levels were measured in brain homogenates. Brain sections at the hippocampus level were processed for H&E and immunohistochemical staining for glial fibrillary acidic protein (GFAP) and amyloid beta (Aβ) 1-42.

Results: Neurodegenerative changes were decreased in subgroups IIc and IId while the most improved histological picture was displayed by IIe. GFAP mean area % and Aβ 1-42 optical density and mean area % decreased in subgroups IIc and IId while the least values were recorded in IIe. Ach-E, GSH and memory test results were ameliorated in subgroups IIc and IId while the best improvement was noticed in IIe.

Conclusion: CO had a prophylactic role against AD. Combination of rivastigmine and CO exerted a great synergistic effect compared to rivastigmine or CO alone.

INTRODUCTION

Alzheimer's disease (AD) is a neurodegenerative disorder which affects memory and cognition[1]. It is characterized by changes in behavior, mood and personality that interfere with a person's daily life and cause a significant burden to families and the healthcare system[2].

The major neuropathological hallmark lesions of AD are cerebral accumulation of extracellular plaques made up of aggregates of amyloid beta (Aβ) protein, intracellular neurofibrillary tangles (NFTs) composed of aggregated microtubule-associated tau proteins, and neuroinflammation[3,4].

Research has focused on the role that aluminum (Al) plays in the changes occurring in AD process[5]. The presence of a high content of Al in rat's brain causes pathological and biochemical changes similar to the alterations observed during AD, such as Aβ aggregation, NFTs, oxidative stress and neuroinflammation[6].

Aluminum chloride ($AlCl_3$)-induced AD rat model is widely used to mimic the pathology of AD and explore its pathophysiology[7,8,9].

The cholinergic system plays an important role in memory and attention. Four drugs have been approved for the treatment of AD patients; the cholinesterase inhibitors (ChE-Is) [donepezil, galantamine, and rivastigmine], and the N-methyl-D-aspartate (NMDA) receptor antagonist, memantine. These drugs slightly improve the cognitive abilities of AD patients, but do not provide a cure. Therefore, disease modifying remedies aiming to pause the progression of AD and alter its pathogenesis, are needed[1,10].

Progressing research studies the role of dietary supplements in ameliorating neurodegenerative impairments. In line with this, it is worth mentioning that AD can be modified by dietary interventions and a healthy life-style[11,12].

Coconut oil (CO) is rich in phenolic compounds, which are recognized for their antioxidant properties. On that account, CO represents an emerging potential approach for prevention and management of AD[13].

This work was designed to evaluate the effect of rivastigmine and CO (alone or together) on $AlCl_3$-induced AD model in the hippocampus of adult male albino rats.

MATERIALS AND METHODS

Drugs

- Aluminum chloride ($AlCl_3$), Aldawlia Company (Cairo, Egypt), in the form of powder in 500 gm weighed package. The required dose was weighed using a digital scale.

- Rivastigmine (Exelon), Novartis pharmaceuticals (Cairo, Egypt), in the form of 1.5 mg capsules. The required dose of the capsule content was weighed using a digital scale.

- Coconut oil (CO), Puritan's Pride (USA), in the form of 1000 mg soft gel capsules. The content of the capsule was obtained with a syringe.

Animals

This study included 33 adult male albino rats with average body weight 200 grams. The rats were bred in Kasr Al-Ainy Animal House according to guidelines of the animal ethical committee of Faculty of Medicine, Cairo University in accordance with institutional review board ethical standards and institutional animal care and use committee (IACUC). Approval number: CU-III-F-16-20. Each group was kept in separate wire cages (50x30x20 cm) with wire mesh covers. Rats were kept at room temperature under constant day/night cycles and fed on standard laboratory rat diet and water ad libitum.

Experimental Design

Control and experimental groups of rats, doses of drugs, duration of administration and time of sacrifice are illustrated in (Table 1).

Table 1: Control and experimental groups of rats, doses of drugs, duration of administration and time of sacrifice

Groups	Subgroups, doses of drugs and duration of administration	Time of sacrifice
Group I (Control) (n=8)	Subgroup Ia:(n=2) Received 0.5 ml sterile saline/day intraperitoneal (i.p) injection for 45 days.	After 45 days
	Subgroup Ib:(n=2) Received 0.5 ml sterile saline/day i.p injection for 45 days, then remained without treatment for 30 days.	After 75 days
	Subgroup Ic:(n=2) Received 0.5 ml sterile saline/day i.p injection for 45 days then, 0.5 ml oral sterile saline/day by gastric gavage for 30 days.	After 75 days
	Subgroup Id:(n=2) Negative control rats remained without treatment for 75 days.	After 75 days
Group II (Experimental) (n=25)	Subgroup IIa: (Alzheimer's) (n=5): Received $AlCl_3$ (100mg/kg/day) = (20mg/day/rat 200g) in 0.5 ml sterile saline i.p. injection for 45 days[14,15].	After 45 days
	Subgroup IIb :(Recovery) (n=5): Received $AlCl_3$ (100mg/kg/day) in 0.5 ml sterile saline i.p. injection for 45 days, then, left without treatment for 30 days.	After 75 days
	Subgroup IIc (Rivastigmine treated) (n=5): Received $AlCl_3$ (100mg/kg/day) i.p. in 0.5 ml sterile saline for 45 days, then, rivastigmine (2.5 mg/kg/day) = (0.5 mg/day/rat 200g) in 0.5ml sterile saline orally by gastric gavage for 30 days[16].	After 75 days
	Subgroup IId (Coconut oil treated) (n=5): Received $AlCl_3$ (100mg/kg/day) i.p. in 0.5 ml sterile saline + CO (5g/kg/day) = (1g/day/rat 200g) orally by gastric gavage for 45 days[17], then, CO only, orally, continued, for 30 days.	After 75 days
	Subgroup IIe (Rivastigmine & coconut oil treated) (n=5): Received $AlCl_3$ (100mg/kg/day) i.p. in 0.5 ml sterile saline + CO (5g/kg/day) orally by gastric gavage for 45 days, then, rivastigmine (2.5 mg/kg/day) + CO, orally, for 30 days.	After 75 days

Experimental Procedure

Body Weight (BW)

The body weight of the rats was measured at the beginning of the experiment (day 1), then at day 45 and at the end of the experiment (day 75), using digital electronic balance.

Memory Assessment (Y-Maze Test)

At the end of experimental periods, all rats were subjected to the memory assessment test, the Y- maze to evaluate the cognitive memory of rats[18]. The test was conducted at the Physiology department, Faculty of Medicine, Cairo University.

It was made of three identical wood arms (40 cm long × 35 cm high × 12 cm width) situated at 120° angles and labeled as A, B, and C. Each rat was positioned individually at the end of one arm and allowed to move freely in the maze throughout a 5-min session. Normally, rats would avoid the most recently entered arm and explore new ones. Consecutive entries into the three different arms (i.e., BCA, CBA, and ABC) were documented and defined as spontaneous alternations. Spontaneous alternation percentage (SAP) was calculated according to the equation: SAP (%) = [(number of alternations)/ (total arm entries − 2)] × 100[19,20].

Laboratory Investigations

The laboratory tests were conducted in the Biochemistry Department, Faculty of Medicine, Cairo University. At the end of experimental periods, blood samples were collected from tail veins of the rats and acetylcholinesterase (Ach-E) level was measured in serum. The following biochemical tests were performed on brain homogenates after sacrifice:

- Acetylcholinesterase (Ach-E) level to demonstrate cholinergic activity[21].

- Glutathione (GSH) concentration: to demonstrate antioxidant activity[22].

Sample preparation (Tissue Homogenate)[23]

The tissues were perfused with phosphate buffered saline (PBS) solution, pH 7.4. The tissues were then homogenized in 5–10 ml cold buffer (i.e., 50 mM potassium phosphate, pH 5.1 mM EDTA) per gram tissue. Centrifugation 10,000 x g for 15 minutes at 4 °C was done. Finally, the supernatant was separated and stored on ice.

Histological Studies

The animals were anaesthetized with ketamine (100mg/kg)/xylazine (10mg/kg) intraperitoneal (i.p.) injection[24].

A thoracotomy was performed and the descending aorta was ligated. The rats were perfused transcardially via the left ventricle with 10% formol saline. A small slit opening was done in the right atrium at the start of perfusion. The perfusion was stopped when the venous return from the right atrium became clear. The objective of this fixation process is to preserve brain tissue quickly and uniformly[25,26].

The brains were dissected out, fixed in 10% formol saline, then serial coronal sections were cut till the hippocampus appeared. The tissues were dehydrated in ascending grades of alcohol, cleared in xylene then embedded into paraffin wax. Paraffin sections of 5 μm thickness were prepared and subjected to the following stains:

1. Hematoxylin & Eosin (H&E) staining[27].

2. Immunohistochemichal staining[28] using the following primary antibodies:

- Glial fibrillary acidic protein (GFAP) antibody to detect the class III intermediate filament protein. GFAP Ab-6 (Clone ASTRO6): A mouse monoclonal antibody (Lab Vision Corporation laboratories, CA 94539, USA, catalogue number MS-1376-P).

- Amyloid beta 1-42(Aβ1-42) antibody to detect amyloid beta protein aggregates and amyloid plaques. Aβ1-42: A rabbit polyclonal antibody (Elabscience Biotechnology Inc.®, USA, Catalog No. E-AB-40074) (Recombinant Beta-amyloid protein 42 protein).

The detection system used was UltraVision (Lab Vision Corporation Laboratories, catalogue number TP-060-HL). It is a broad-spectrum system that reacts with mouse and rabbit primary antibodies. The GFAP immunopositive cells show brown cytoplasmic reaction and the amyloid beta 1-42 immunopositive aggregates and plaques show brown immunoreactivity.

Morphometric Studies

Data were obtained using "Leica Qwin 500 C" image analyzer computer system Ltd. (Cambridge, England). The measurements were done in 10 non-overlapping, randomly chosen fields in each section at 400 magnification. The following parameters were measured:

1. Mean area percent of GFAP immunopositive cells.

2. Mean optical density of Aβ1-42 immunopositive plaques.

3. Mean area percent of Aβ1-42 immunopositive plaques.

Statistical Analysis

The measurements obtained were analyzed using Statistical Package for Social Sciences (SPSS) software version 23 (SPSS, Chicago, IL). Comparison between different groups was made using analysis of variance (ANOVA) followed by post hoc Tukey test. The results were expressed as means ± standard deviation (SD). The differences were considered statistically significant when "*p*" was < 0.05[29].

RESULTS

Body Weight, Memory Assessment and Laboratory results

These are illustrated in (Tables 2, 3 respectively).

Histological Results

I- Hematoxylin and Eosin

Group I (control group) sections showed the same histological picture of a normal rat hippocampus in the four subgroups, (Ia, Ib, Ic and Id). The hippocampus was formed of Cornu Ammonis (CA) and the dentate gyrus (DG). Cornu Ammonis was formed of four areas, CA1 and CA2 in the superior region, and CA3 and CA4 in the inferior

region. The CA layers from external to internal were: the alveus (Alv), stratum oriens (SO), stratum pyramidale (SP), stratum radiatum (SR) and stratum lacunosum-moleculare (SLM). The stratum lucidum (SL) was only present in CA3 region. The DG appeared as a C-shaped structure with an upper limb (UL) and a lower limb (LL). The DG layers were arranged as: stratum moleculare (SM), stratum granulosum (SG) and polymorphic layer (PL). The CA4 was situated within the concavity of the DG which formed the hilus (H) (Figure 1A,B).

The SP was the principal layer of CA. It was formed of closely arranged small pyramidal cells with large rounded vesicular nuclei, prominent nucleoli and basophilic cytoplasm in CA1. In CA3, SP was formed of large pyramidal cells. The SL was formed of Mossy fibers compressed between SP and SR. The SO contained the basal dendrites of the pyramidal neurons while SR contained their apical dendrites. The SG was the main layer of the DG. It contained granular neurons, which were small, round and densely packed with rounded vesicular nuclei, prominent nucleoli and basophilic cytoplasm. The dendrites of the granular cells were located in SM, while their axons "Mossy fibers" ran in PL. Blood vessels and glial cells were detected (Figure 2A-C).

Sections from subgroups IIa and IIb revealed marked changes in CA1, CA3 and DG. In CA1, most of the pyramidal cells in SP were degenerated, while in CA3, multiple degenerated shrunken pyramidal cells were detected in subgroup IIa and many were seen in subgroup IIb. They displayed loose irregular arrangement, deformed morphology with pyknotic nuclei, darkly stained cytoplasm and pericellular halos. Few intact pyramidal cells with vesicular nuclei, prominent nucleoli and basophilic cytoplasm were seen in subgroup IIa while in subgroup IIb, sparse intact cells were observed in CA1 and some were detected in CA3. Vacuolations in the neuropil, glial cells with pyknotic nuclei and blood vessel dilatation were noticed. The UL of the DG showed many shrunken granular cells with pyknotic nuclei in SG. Some intact granular cells with vesicular nuclei, prominent nucleoli and basophilic cytoplasm were seen. Wide areas of vacuolation in the neuropil and glial cells with pyknotic nuclei were observed (Figure 3A-F).

Sections from subgroups IIc and IId showed regularly arranged intact pyramidal cells with vesicular nuclei, prominent nucleoli and basophilic cytoplasm in SP of CA1 and CA3. Few degenerated shrunken dark pyramidal cells with pyknotic nuclei were observed in subgroup IIc, as for subgroup IId, some degenerated cells were seen in CA1 while few ones were detected in CA3. The UL of the DG showed intact granular neurons in SG with vesicular nuclei, prominent nucleoli and basophilic cytoplasm. Some degenerated shrunken cells with pyknotic nuclei were noticed in subgroup IIc while many ones were seen in subgroup IId. Vacuolations in the neuropil were observed. Few glial cells with pyknotic nuclei were also detected (Figure 4A-F).

Subgroup IIe showed regularly arranged intact pyramidal cells with vesicular nuclei, prominent nucleoli and basophilic cytoplasm in SP of CA1 and CA3. Sparse degenerated shrunken dark cells with pyknotic nuclei were detected in CA1 while occasional ones were noticed in CA3. The UL of the DG showed intact granular neurons in SG with vesicular nuclei, prominent nucleoli and basophilic cytoplasm. Few degenerated shrunken cells with pyknotic nuclei were noticed. Vacuolations in the neuropil were noticed. Few glial cells with pyknotic nuclei were also observed (Figure 5A-C).

II- Anti-GFAP Immunostained Sections

Group I (control group) sections showed the same histological picture in the four subgroups (Ia, Ib, Ic and Id). They revealed positive brown immunostaining in the cytoplasm and processes of astrocytes in SO, SP and SR of CA1 and CA3 as well as SM, SG and PL of the UL of the DG (Figure 6A-C).

Sections from subgroups IIa and IIb revealed strong positive brown immunoreaction in many astrocytes in SO, SP and SR of CA1 and CA3. Similarly, the immunostaining was detected in many astrocytes in SM, SG and PL of the UL of the DG. The close relation of the strongly immunopositive astrocytes to the degenerated neurons was observed (Figure 7A-F).

Subgroups IIc and IId sections revealed reduced immunoreaction as compared to subgroups IIa and IIb. Moderate positive immunostaining was detected in astrocytes in SO, SP and SR of CA1 and CA3 as well as in SM, SG and PL of the UL of the DG (Figure 8A-F).

Reduced immunoreaction was seen in sections from subgroup IIe when compared to subgroups IIa and IIb. Moderate positive immunostaining was detected in astrocytes in SO, SP and SR of CA1 and CA3. Mild brown immunostaining was observed in the astrocytes in SM, SG and PL of the UL of the DG (Figure 9A-C).

III- Anti-Aβ 1-42 Immunostained Sections

Group I (control group) sections showed the same histological picture in the four subgroups (Ia, Ib, Ic and Id). They revealed negative immunoreaction through the layers SO, SP and SR in CA1 and CA3 as well as the layers SM, SG and PL of the UL of the DG (Figure 10A-C).

Strong positive immunoreaction was revealed in sections from subgroups IIa and IIb. Multiple strong positive immunostained amyloid plaque was observed as dense brown immunostained deposits in SR layer of CA1 and CA3 in addition to ones near blood vessels, as well as in SM layer of UL of the DG (Figure 11A-F).

Sections from subgroups IIc and IId revealed moderate positive immunoreaction. Some moderate positive immunostained amyloid plaques were observed in SR layer of CA1 and few in CA3. Also, amyloid plaques were observed near blood vessels. In subgroup IIc many moderate positive immunostained amyloid plaques were

seen in SM layer of UL of the DG while multiple ones were noticed in subgroup IId (Figure 12A-F).

Weak positive immunoreaction was noticed in sections from subgroup IIe. Faint brown immunostaining was detected in SR layer of CA1 and CA3 but no plaques were detected in both areas. While, few mild positive immunostained amyloid plaques were observed in SM layer of the UL of the DG (Figure 13A-C).

## Morphometric Results

These are illustrated in (Table 4).
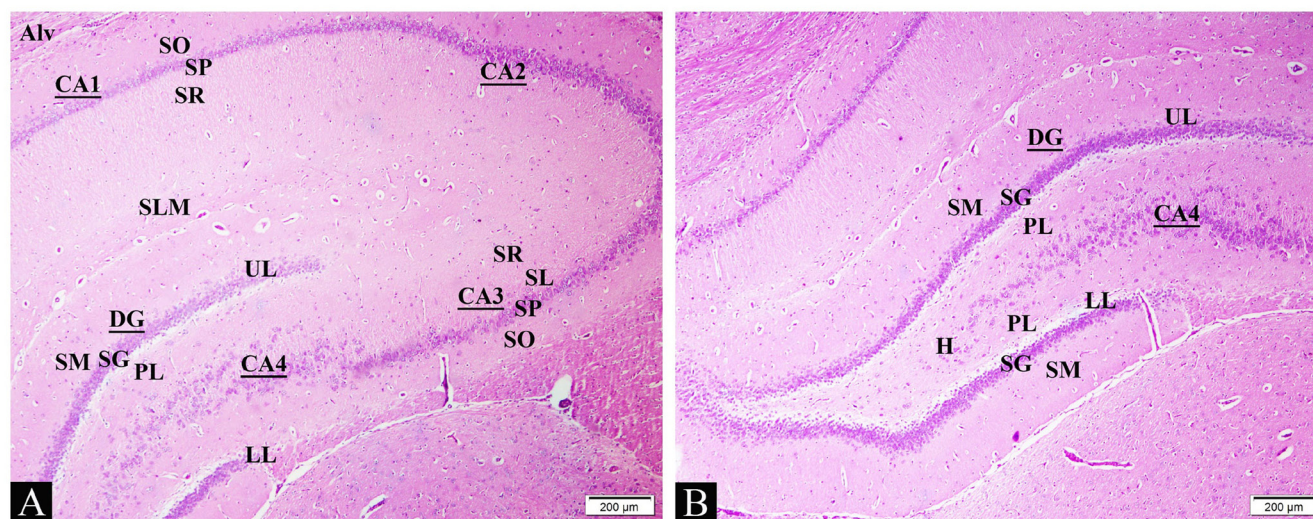
Fig. 1: Photomicrograph of sections in the hippocampus from group I (control group) showing: A: Cornu Ammonis is formed of CA1, CA2, CA3 and CA4. The CA layers are: the alveus (Alv), stratum oriens (SO), stratum pyramidale (SP), stratum radiatum (SR) and stratum lacunosum-moleculare (SLM). The stratum lucidum (SL) is only present in CA3. B: The dentate gyrus (DG) has an upper (UL) and a lower limb (LL). It is formed of: stratum moleculare (SM), stratum granulosum (SG) and polymorphic layer (PL). The concavity of the DG forms the hilus (H) where CA4 is situated. (H&E, x40).
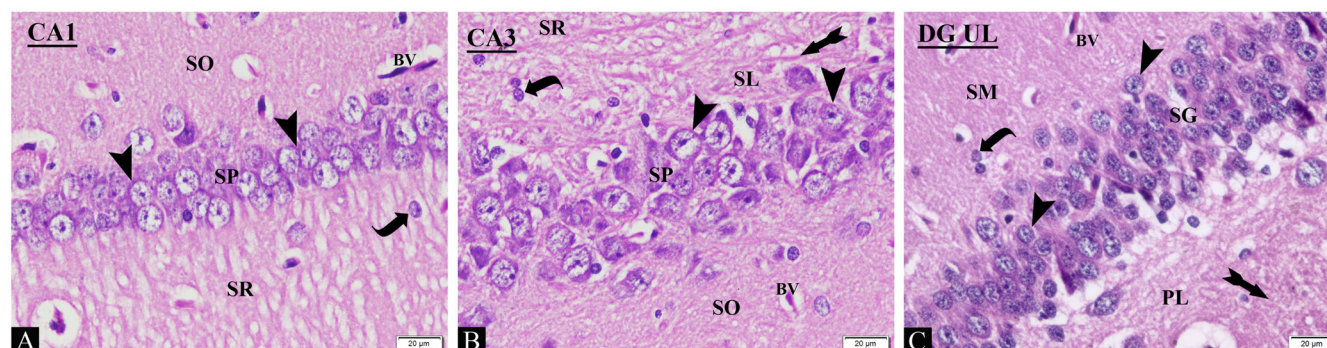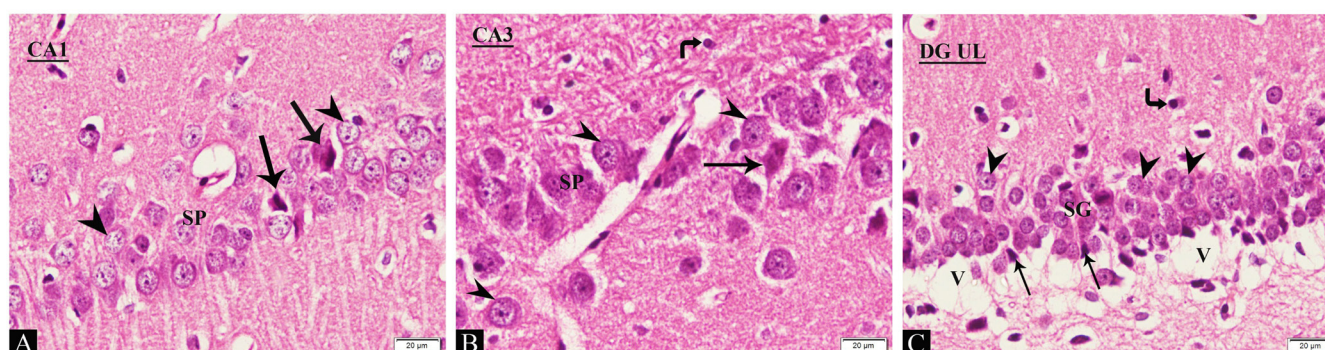

Fig. 2: Photomicrograph of sections in the hippocampus from group I (control group) in: A: CA1 showing SP formed of closely arranged pyramidal cells with large rounded vesicular nuclei, prominent nucleoli and basophilic cytoplasm (arrow heads). SO contains the basal dendrites of the pyramidal neurons and SR contains their apical dendrites. Blood vessels (BV) and glial cells (curved arrow) are detected. B: CA3 showing SP formed of large pyramidal cells with large rounded vesicular nuclei, prominent nucleoli and basophilic cytoplasm (arrow heads). SO and SR contain the dendrites of the pyramidal neurons. Blood vessels (BV) and glial cells (curved arrow) are seen. Mossy fibers are detected (bifid arrow) in SL. C: UL of DG showing SG. It contains granular neurons which are small, densely packed with rounded vesicular nuclei, prominent nucleoli and basophilic cytoplasm (arrow heads). Their dendrites are present in SM, while their axons "Mossy fibers" (bifid arrow) are in PL. Blood vessels (BV) and glial cells (curved arrow) are observed. (H&E, x400).
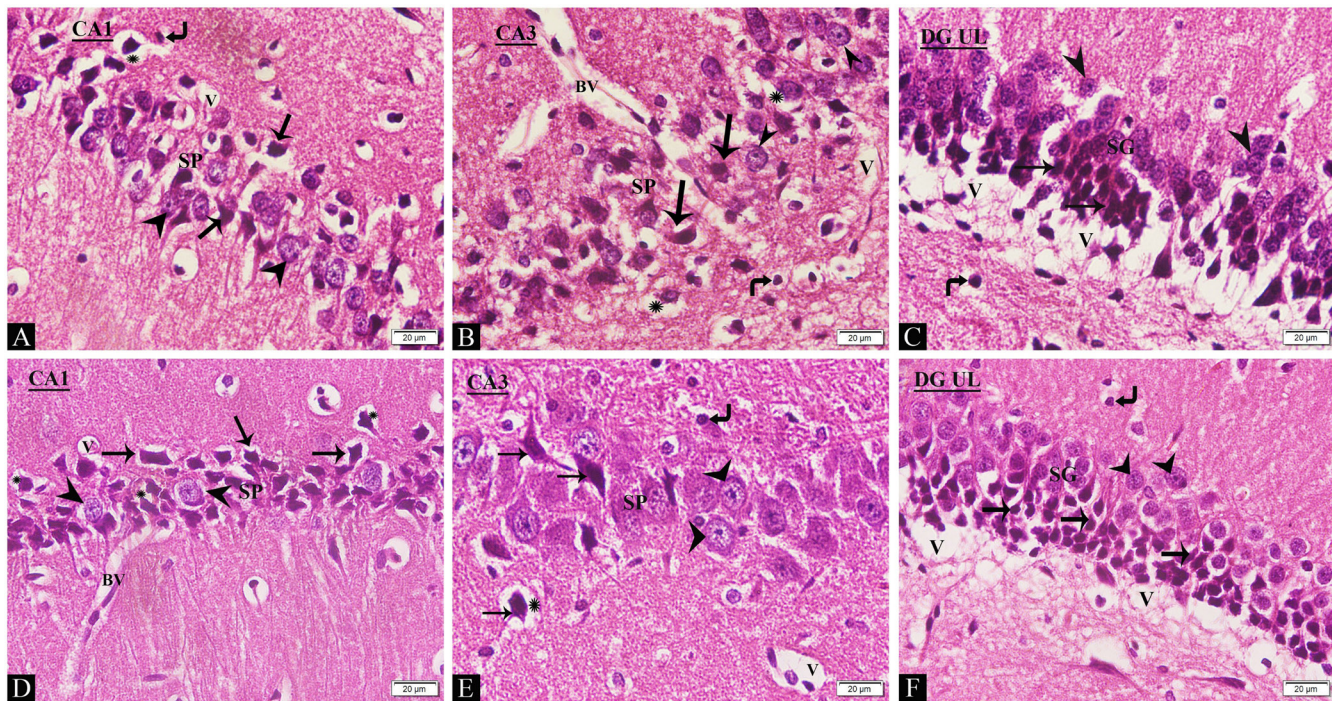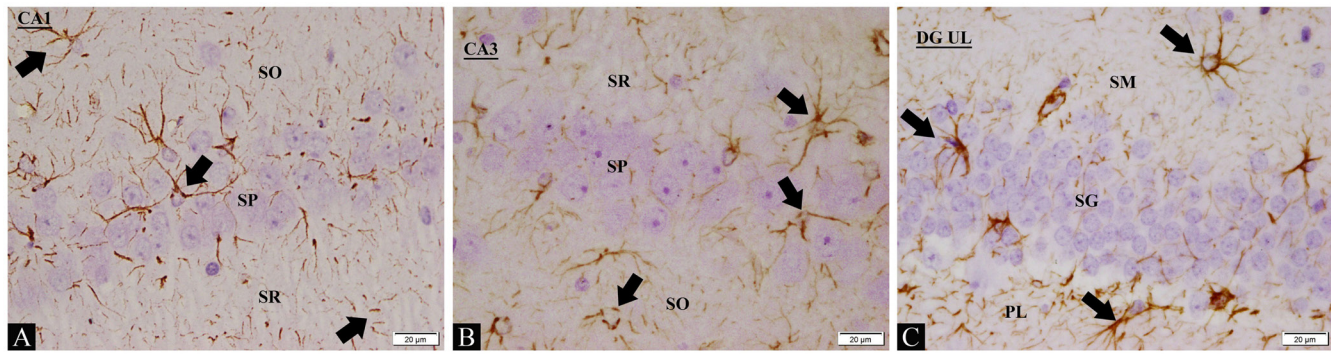
Fig. 3: Photomicrograph of sections in the hippocampus. A, B & C: from subgroup IIa (Alzheimer's group); D, E & F: from subgroup IIb (recovery group). A: CA1 showing most of the loosely arranged pyramidal cells in SP are shrunken with pyknotic nuclei and darkly stained cytoplasm (arrows) in addition to the presence of pericellular halos (*). Few intact pyramidal cells with vesicular nuclei, prominent nucleoli and basophilic cytoplasm (arrow heads), glial cells with pyknotic nuclei (right angle arrow) and vacuolations (V) in the neuropil are detected. B: CA3 showing multiple pyramidal cells (arrows) in SP displaying an irregular arrangement with deformed morphology, pyknotic nuclei and darkly stained cytoplasm. Pericellular halos (*) are also observed. Few intact pyramidal cells with vesicular nuclei, prominent nucleoli and basophilic cytoplasm (arrow heads) and glial cells with pyknotic nuclei (right angle arrow) are seen. Vacuolations (V) in the neuropil and blood vessel (BV) dilatation are noticed. C: UL of DG show many shrunken granular cells with pyknotic nuclei (arrows) in SG. Some intact granular cells with vesicular nuclei, prominent nucleoli and basophilic cytoplasm (arrow heads) are seen. Glial cells with pyknotic nuclei (right angle arrow) and wide areas of vacuolation (V) in the neuropil are observed. D: CA1 showing most of the pyramidal cells in SP display an irregular arrangement with deformed morphology, pyknotic nuclei and darkly stained cytoplasm (arrows), in addition to pericellular halos (*). Sparse intact pyramidal cells with vesicular nuclei, prominent nucleoli and basophilic cytoplasm (arrow heads) are noticed, in addition to vacuolations (V) in the neuropil and blood vessel (BV) dilatation. E: CA3 showing many shrunken irregularly arranged pyramidal cells with pyknotic nuclei, and darkly stained cytoplasm (arrows) in SP with pericellular halos (*). Some intact pyramidal cells with vesicular nuclei, prominent nucleoli and basophilic cytoplasm (arrow heads), glial cells with pyknotic nuclei (right angle arrow) and vacuolations (V) in the neuropil are seen. F: UL of DG showing many granular cells with pyknotic nuclei (arrows) in SG. Some intact granular cells with vesicular nuclei, prominent nucleoli and basophilic cytoplasm (arrow heads), glial cells with pyknotic nuclei (right angle arrow) and wide areas of vacuolations (V) are observed. (H&E, x400).
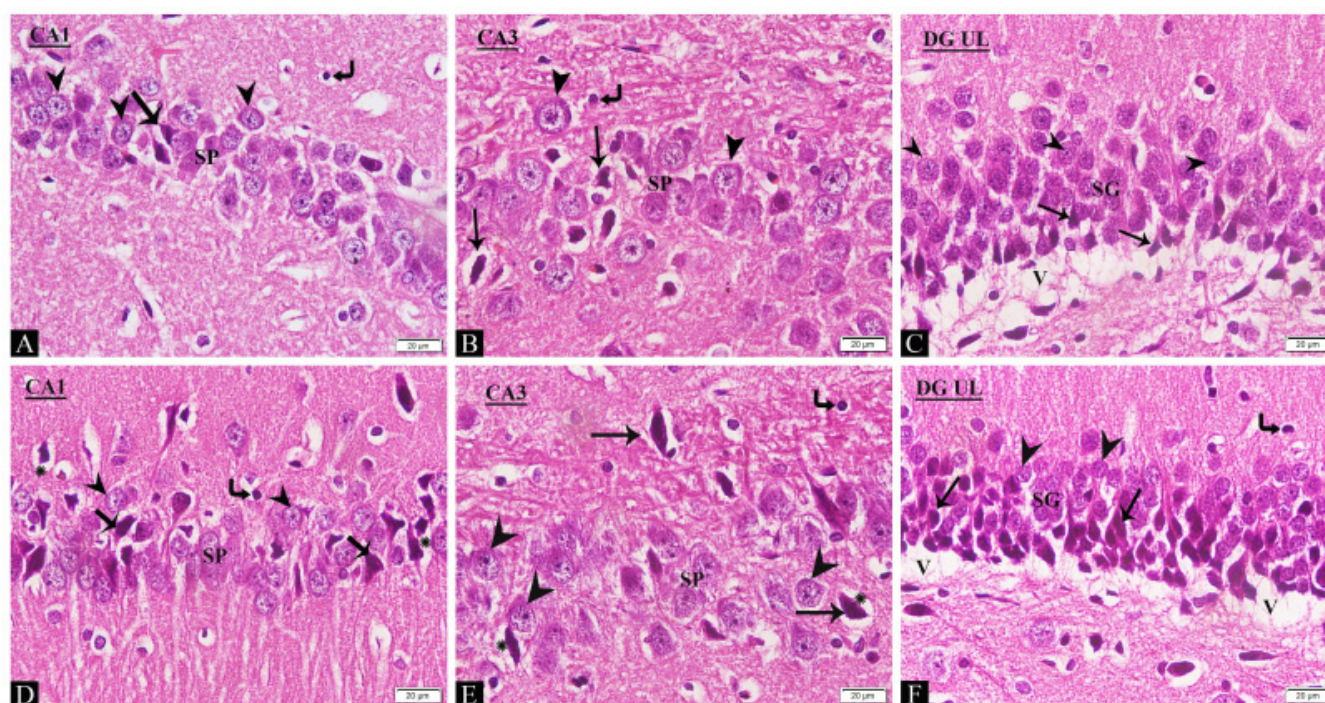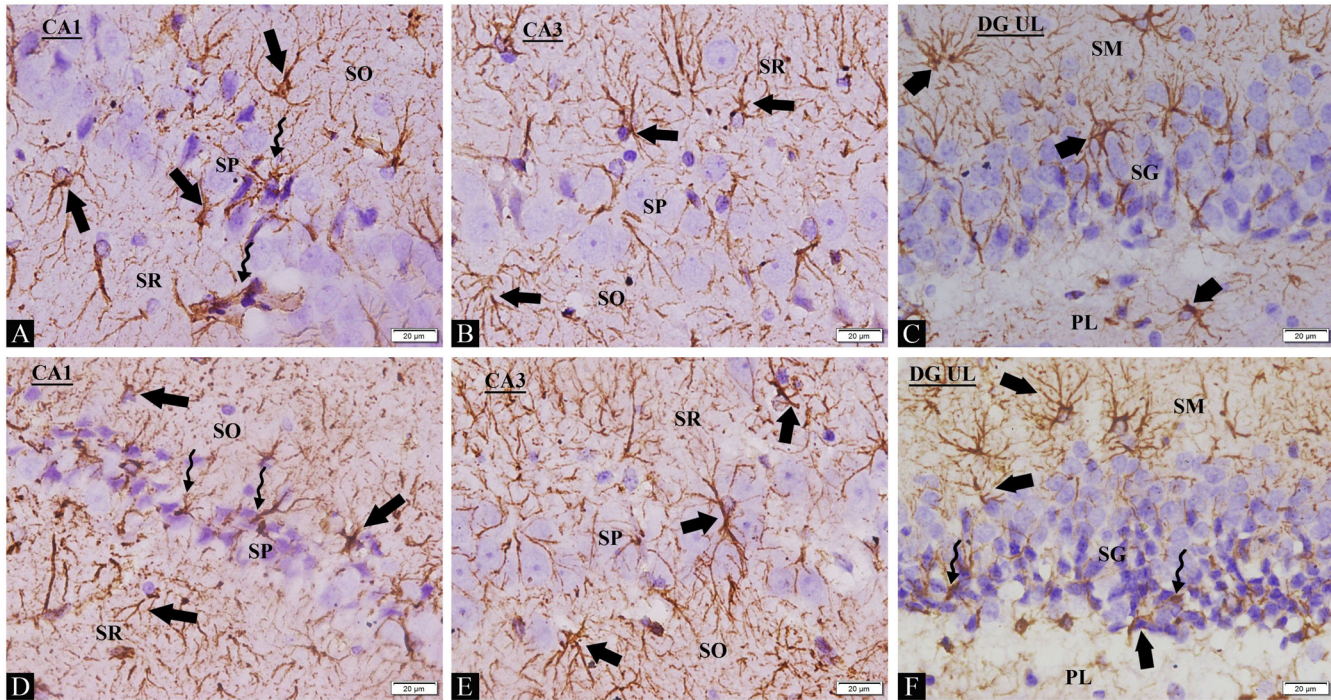
Fig. 4: Photomicrograph of sections in of the hippocampus. A, B & C: from subgroup IIc (rivastigmine treated group); D, E & F: from subgroup IId (CO treated group). A: CA1 showing regularly arranged intact pyramidal cells with vesicular nuclei, prominent nucleoli and basophilic cytoplasm (arrow heads) in SP. Few degenerated shrunken dark cells with pyknotic nuclei (arrow) and glial cells with pyknotic nuclei (right angle arrow) are detected. B: CA3 showing large pyramidal cells with vesicular nuclei, prominent nucleoli and basophilic cytoplasm (arrow heads) in SP. Few degenerated cells with pyknotic nuclei and darkly stained cytoplasm (arrows) and glial cells with pyknotic nuclei (right angle arrow) are noticed. C: UL of DG showing intact granular neurons with vesicular nuclei, prominent nucleoli and basophilic cytoplasm (arrow heads) in SG. Some degenerated shrunken cells with pyknotic nuclei (arrows) are seen. Vacuolations (V) in the neuropil are observed. D: CA1 showing regularly arranged intact pyramidal cells with vesicular nuclei, prominent nucleoli and basophilic cytoplasm (arrow heads) in SP. Some shrunken cells with pyknotic nuclei, darkly stained cytoplasm (arrows) and pericellular halos (*), as well as few glial cells with pyknotic nuclei (right angle arrow) are noticed. E: CA3 showing large intact pyramidal cells with vesicular nuclei, prominent nucleoli and basophilic cytoplasm (arrow heads) in SP. Few shrunken dark cells with pyknotic nuclei (arrows) and pericellular halos (*), in addition to glial cells with pyknotic nuclei (right angle arrow) are seen. F: UL of DG showing intact granular neurons (arrow heads) with vesicular nuclei, prominent nucleoli and basophilic cytoplasm in SG. Many degenerated shrunken cells with pyknotic nuclei (arrows) are seen. Vacuolations (V) in the neuropil and few glial cells with pyknotic nuclei (right angle arrow) are also observed. (H&E, x400).
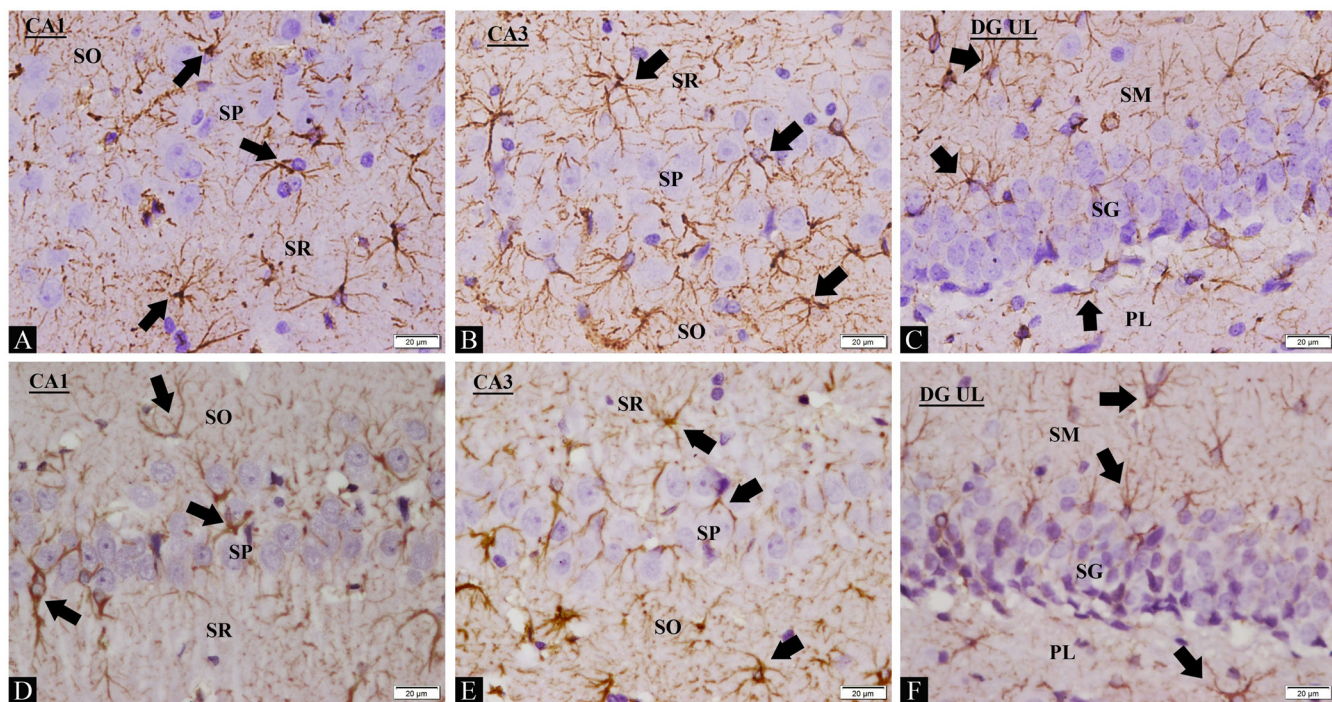

Fig. 5: Photomicrograph of sections of the hippocampus from subgroup IIe (rivastigmine and CO treated group) in: A: CA1 showing regularly arranged intact pyramidal cells with vesicular nuclei, prominent nucleoli and basophilic cytoplasm (arrow heads) in SP. Sparse degenerated shrunken dark cells with pyknotic nuclei (arrows) are observed. B: CA3 showing large intact pyramidal cells with vesicular nuclei, prominent nucleoli and basophilic cytoplasm (arrow heads) in SP. One degenerated, shrunken and darkly stained cell with pyknotic nucleus (arrow) is noticed. Few glial cells with pyknotic nuclei (right angle arrow) are also seen. C: UL of DG showing intact granular neurons with vesicular nuclei, prominent nucleoli and basophilic cytoplasm (arrow heads) in SG. Few degenerated shrunken cells with pyknotic nuclei (arrows), glial cells with pyknotic nuclei (right angle arrow) and vacuolations (V) in the neuropil are detected. (H&E, x400).
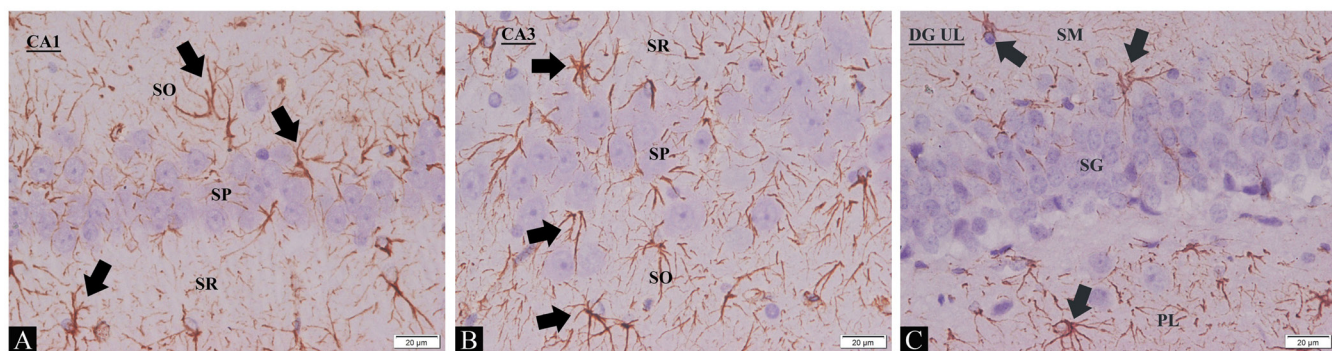
Fig. 6: Photomicrograph of sections in the hippocampus from group I (control group) in; A: CA1 and B: CA3 showing positive brown immunostaining in the cytoplasm and processes of astrocytes (thick arrows) in SO, SP and SR. C: UL of DG showing positive brown immunoexpression in the cytoplasm and processes of astrocytes (thick arrows) in SM, SG and PL. (Anti-GFAP Immunostaining, x400).
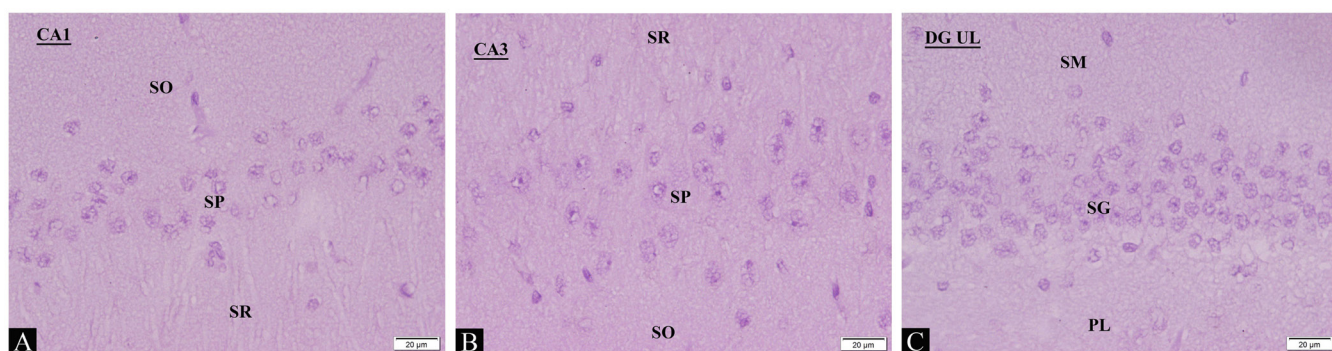

Fig. 7: Photomicrograph of sections of the hippocampus. A, B & C: from subgroup IIa (Alzheimer's group); D, E & F: from subgroup IIb (recovery group). A: CA1 and B: CA3 show strong positive brown immunoreaction in many astrocytes (thick arrows) in SO, SP and SR. Note in A, the close relation of the strongly immunopositive astrocytes to the degenerated neurons (wavy arrows). C: UL of DG showing strong positive brown immunoexpression in many astrocytes (thick arrows) in SM, SG and PL. D: CA1 and E: CA3 show strong positive brown immunostaining in many astrocytes (thick arrows) in SO, SP and SR. Note in D, the strongly immunopositive astrocytes closely related to the degenerated neurons (wavy arrows). F: UL of DG showing strong positive brown immunoreaction in many astrocytes (thick arrows) in SM, SG and PL. The close relation of the strongly immunopositive astrocytes to the degenerated neurons (wavy arrows) is observed. (Anti-GFAP Immunostaining, x400).
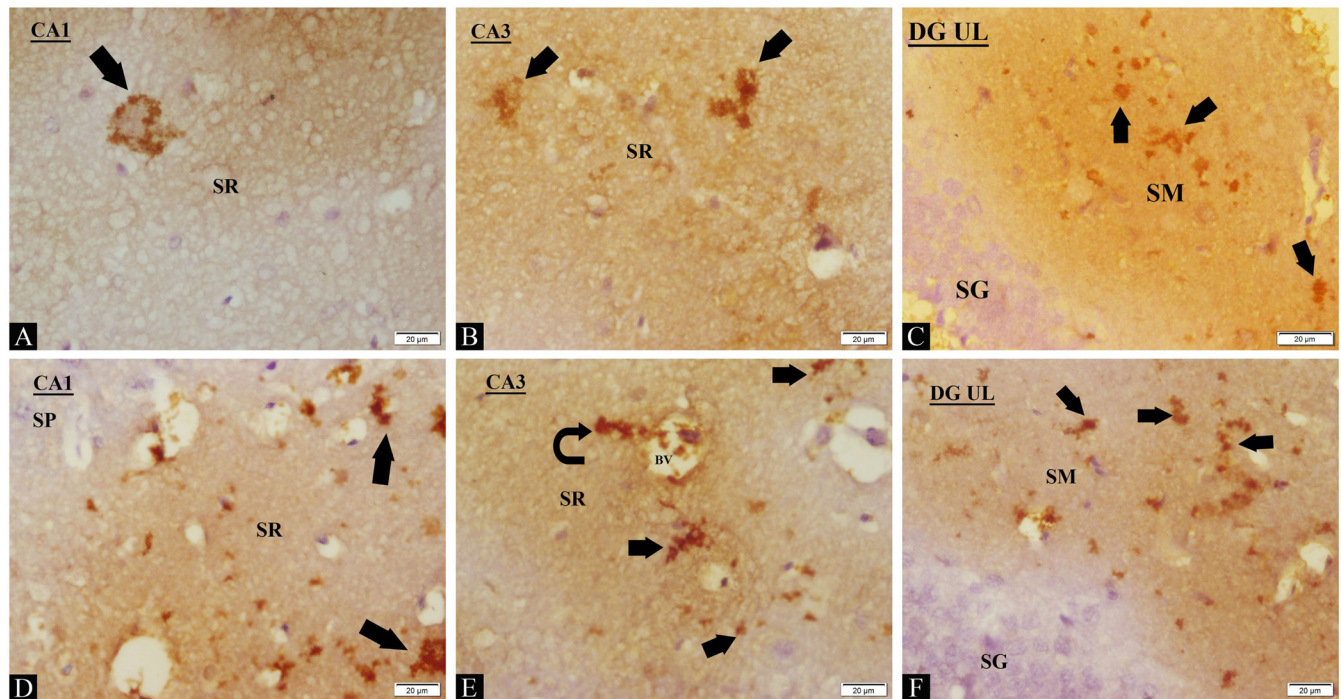
Fig. 8: Photomicrograph of sections of the hippocampus. A, B & C: from subgroup IIc (rivastigmine treated group); D, E & F: from subgroup IId (CO treated group). A: CA1 and B: CA3 show moderate brown positive immunoreaction in the astrocytes (thick arrows) in SO, SP and SR. C: UL of DG showing moderate positive brown immunostaining in the astrocytes (thick arrows) in SM, SG and PL. D: CA1 and E: CA3 show moderate positive brown immunoreactivity in the astrocytes (thick arrows) in SO, SP and SR. F: UL of DG showing moderate positive brown immunostaining in of astrocytes (thick arrows) in SM, SG and PL. (Anti-GFAP Immunostaining, x400).
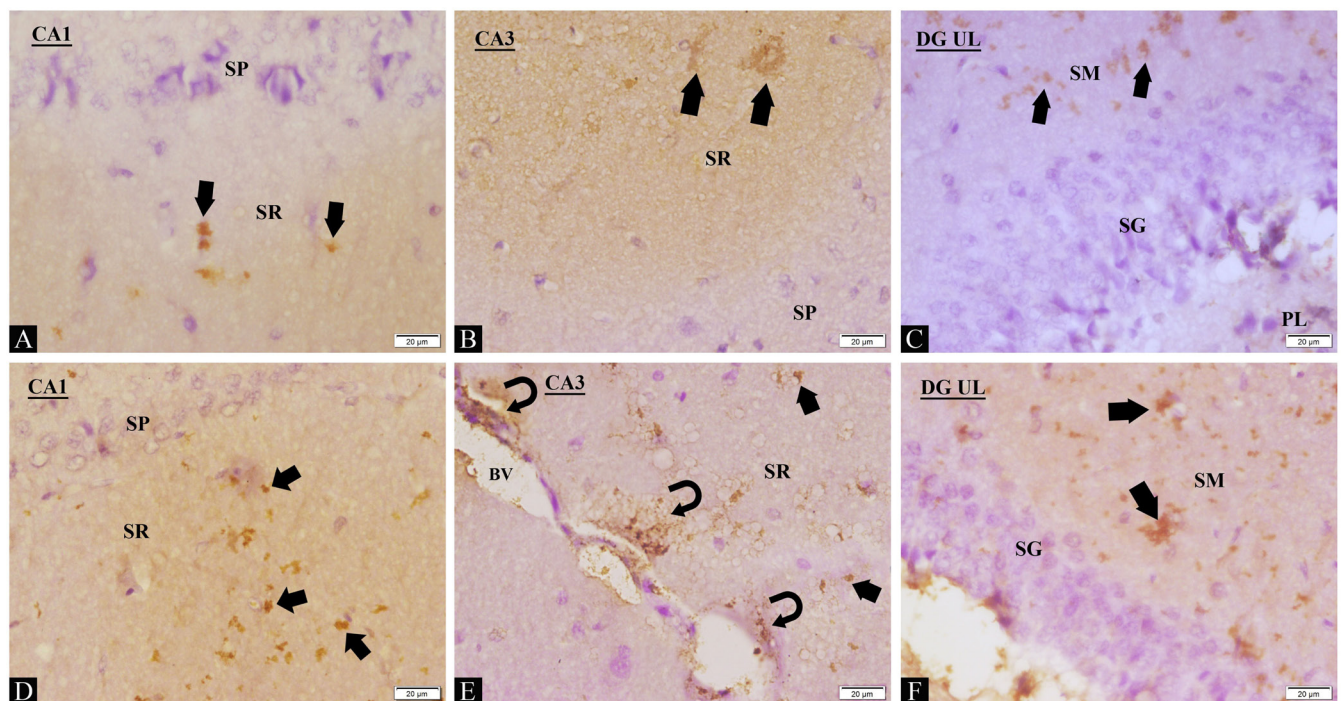

Fig. 9: Photomicrograph of sections of the hippocampus from subgroup IIe (rivastigmine and CO treated group) in A: CA1 and B: CA3 show moderate brown immunoexpression in the astrocytes (thick arrows) in SO, SP and SR. C: UL of DG showing mild brown immunoreactivity in the astrocytes (thick arrows) in SM, SG and PL. (Anti-GFAP Immunostaining, x400).
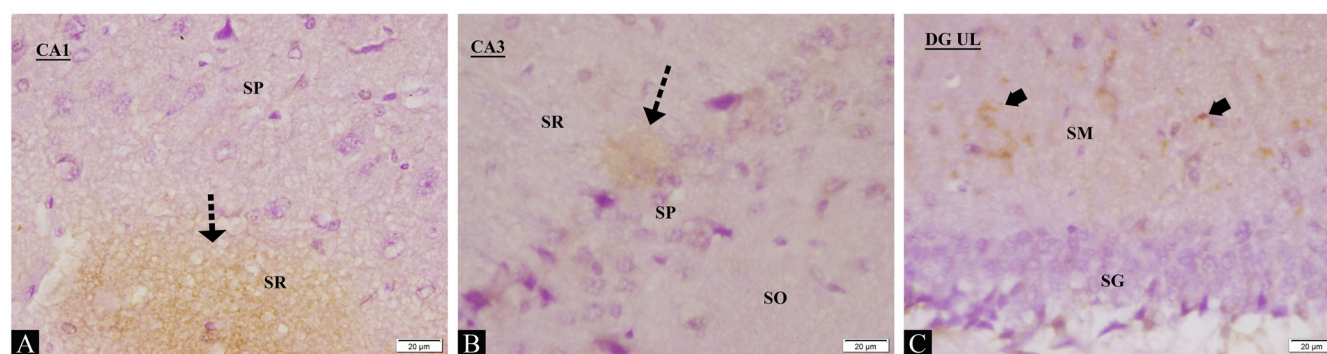

Fig. 10: Photomicrograph of sections of the hippocampus from group I (control group) in A: CA1 and B: CA3 showing negative immunoreaction through the layers SO, SP and SR. C: UL of DG showing negative immunoreactivity in SM, SG and PL. (Aβ1-42 Immunostaining, x 400).

Fig. 11: Photomicrograph of sections of the hippocampus. A, B & C: from subgroup IIa (Alzheimer's group); D, E & F: from subgroup IIb (recovery group) showing strong positive immunoexpression. A: CA1 showing strong positive immunostained amyloid plaque in SR which appear as dense brown immunostained deposits (thick arrow). B: CA3 showing multiple strong positive immunostained amyloid plaques in SR which appear as dense brown immunostained deposits (thick arrows). C: UL of DG showing multiple strong positive immunostained amyloid plaques in SM (thick arrows). SG is noticed. D: CA1 showing multiple strong positive immunostained amyloid plaques in SR (thick arrows). SP is noticed. E: CA3 showing multiple strong positive immunostained amyloid plaques in SR (thick arrows). Amyloid plaques (curved arrow) are detected near a blood vessel (BV). F: UL of DG showing multiple strong positive immunostained amyloid plaques in SM (thick arrows). SG is seen. (Aβ1-42 Immunostaining, x 400).

Fig. 12: A Photomicrograph of sections of the hippocampus. A, B & C: from subgroup IIc (rivastigmine treated group); D, E & F: from subgroup IId (CO treated group) showing moderate positive immunoreaction. A: CA1 showing some moderate positive immunostained amyloid plaques in SR (thick arrows). SP is noticed. B: CA3 showing few immunostained amyloid plaques in SR (thick arrows). SP is seen. C: UL of DG showing many immunostained amyloid plaques in SM (thick arrows). SG and PL are noticed. D: CA1 showing some moderate positive immunostained amyloid plaques in SR (thick arrows). SP is observed. E: CA3 showing few immunostained amyloid plaques in SR (thick arrows). Amyloid plaques (curved arrows) are observed near blood vessel (BV). F: UL of DG showing multiple immunostained amyloid plaques in SM (thick arrows). SG is noticed. (Aβ1-42 Immunostaining, x 400).

Fig. 13: Photomicrograph of sections of the hippocampus from subgroup IIe (rivastigmine and coconut oil treated group) showing weak positive immunoreaction. A: CA1 showing faint brown immunostaining in SR (dotted arrow) but no plaques are detected. SP is noticed. B: CA3 showing faint brown immunostaining (dotted arrow) in SR. Note the absence of plaques. SP and SO are seen. C: UL of DG showing few mild positive immunostained amyloid plaques in SM (thick arrows). SG is noticed. (Aβ1-42 Immunostaining, x 400).

Table 2: The mean values ± SD of the BW of control and experimental groups at day1, 45 and 75.

Group	day 1	day 45	day 75
I	200±1.61	240±1.58	291.6±3.91
IIa	198.8±4.32	156.7±2.33*	-
IIb	204±4.52	162±8.54*	191.4±9.52#
IIc	197±7.52	168.6±16.86*	250±18.7#γ
IId	205±1.27	210.6±3.2*□	262.8±15.93#γ
IIe	200.2±4.44	215.2±1.92*□	266.8±9.3#γ

*Significant compared to group I at day 45 ($p < 0.05$).   □Significant compared to subgroups IIa, IIb, IIc at day 45($p < 0.05$).

#Significant compared to group I at day 75 ($p < 0.05$).   γSignificant compared to subgroup IIb at day 75 ($p < 0.05$).

Table 3: The mean values ± SD of SAP %, Ach-E enzyme in serum, and Ach-E and GSH in brain homogenates of control and experimental

groups.

Group	SAP%	Serum Ach-E (U/ml)	Brain Ach-E (U/mg tissue)	Brain GSH (mmol/mg tissue)
I	84.42±2.84	13.06±0.54	24.02±0.39	57.4±0.76
IIa	40.5±3.02*	22.72±0.84*	43.26±1.88*	39.1±0.79*
IIb	33.28±1.08*	31.6±0.76*○	48.18±0.67*○	32.7±0.98*○
IIc	70.5±4.18*Δ	15.92±0.94*Δ	29.78±1.34*Δ	53.64±2.22*Δ
IId	67±2.52*Δ	16.82±2.42*Δ	30.9±1.62*Δ	52.96±2.95*Δ
IIe	74.31±7.48*Δ	14.9±2.06Δ	27.28±4.71Δ	55.6±0.72Δ

* Significant compared to group I ($p < 0.05$).   Δ Significant compared to subgroups IIa and IIb ($p < 0.05$).   ○ Significant compared to subgroup IIa ($p < 0.05$).

Table 4: The mean values ±SD of area % of GFAP immunopositive cells, and optical density and area % of Aβ 1-42 immunopositive plaques

in control and experimental groups.

Group	GFAP mean area%	Aβ1-42 optical density	Aβ mean area%
I	3.14±0.23	0	0
IIa	12.94±0.46*	0.283±0.039*	7.77±1.34*
IIb	14.94±0.89*	0.31±0.026*	9.078±1.52*
IIc	7.64±0.85*Δ	0.13±0.021*Δ◊	3.19±0.84*Δ◊
IId	8.92±4.61*Δ	0.17±0.023*Δ	5.38±0.84*Δ
IIe	5.3±2.7Δ	0.083±0.01*Δ•	0.92±0.38*Δ•

* Significant compared to group I ($p < 0.05$).   Δ Significant compared to subgroups IIa and IIb ($p < 0.05$).
◊ Significant compared to subgroup IId ($p < 0.05$).   • Significant compared to subgroups IIc and IId ($p < 0.05$).

DISCUSSION

The purpose of the current study was to evaluate the effect of rivastigmine and CO (alone or together) on $AlCl_3$-induced AD model in the hippocampus of adult male albino rats.

The hippocampus is a vulnerable area in the brain associated with memory and cognition. Therefore, its damage is involved in the progression of AD[30]. AD is characterized by progressive neurodegeneration, which initiates neuronal death in CA1 region, then CA3 area of the hippocampus[31]. Area CA2 is relatively highly resistant to injury compared with other CA regions[32] while DG is early exposed to alterations in vascular permeability related to AD[33].

Accordingly, CA1, CA3 and DG of the hippocampus were chosen to study the changes after induction of AD.

Aluminum stimulates the production of free radicals in the brain that leads to neurodegenerative features such as Aβ accumulation, neuroinflammation and neuronal necrosis, similar to those that characterize AD[34,35]. The $AlCl_3$-induced AD rat model was used in numerous studies to mimic the pathological changes of AD[36,37,38]. The $AlCl_3$ dose selected in this work was correlated to individuals who are liable to exposure to dangerous levels of Al, for example occupational Al toxicity[20] as such high dose was reported to cause deposition of amyloid plaques[39].

In the current study, $AlCl_3$ exposure (after 45 days) caused a significant reduction in the BW in group II (experimental) in all its subgroups IIa, IIb, IIc, IId and IIe as compared to group I (control group). Lack of desire for food and water intake was observed which explained the weight loss. Findings previously recorded by Justin-Thenmozhi *et al.* (2015)[40] and Yang *et al.* (2020)[38] were in agreement with our results as they also reported decreased BW in rat models during $AlCl_3$ exposure. Furthermore, Olajide *et al.* (2017)[18] described weight decline as a metabolic dysfunction observed in AD.

Coconut oil administration with $AlCl_3$ in rats of subgroups IId and IIe significantly improved the BW gain compared to the $AlCl_3$ induced AD rats (subgroups IIa and IIb) in addition to rivastigmine treated rats (subgroup IIc). This could be explained by preserved appetite and food consumption due to CO which suggests a prophylactic role for CO against the $AlCl_3$-induced metabolic imbalance.

At the end of the experiment (after 75 days), $AlCl_3$ exerted significant decrease in BW of experimental subgroups compared to control. However, the treated subgroups with CO and rivastigmine alone or together (IIc, IId and IIe) have regained their BW and it significantly improved compared to subgroup IIb (recovery subgroup treated with $AlCl_3$ only). This could be attributed to observed gradual regain of appetite and increased food consumption. Likewise, Upadhyaya *et al.* (2019)[41] reported that rivastigmine treatment resulted in regain of BW of $AlCl_3$-treated rats. Regarding CO intake, Olanrewaju *et al.* (2018)[42] reported that CO administration resulted in regain of BW of $AlCl_3$-treated rats.

The Y-Maze test is regarded as a functional index of the cortex and hippocampus as it has been utilized in experimental studies related to cognitive impairment in rats[43].

In the current study, spontaneous alteration percentage (SAP%) in all experimental subgroups significantly decreased compared to control group due to exposure to $AlCl_3$. These results were consistent with the findings of Alawdi *et al.* (2017)[44] who demonstrated that Al lowered the SAP% in Y-maze test significantly as compared to normal rats group.

Aluminum adversely affects the mammalian central nervous system (CNS). It impairs the enzymes related to neurotransmitter synthesis. It also inhibits neurotransmitter receptors and delays synaptic transmission, which all are manifested in spatial memory deficit[34].

In the present study, significant increase of SAP% in subgroups IIc, IId and IIe (rivastigmine and CO treated groups) was observed as compared to subgroups IIa and IIb. Similar findings were reported by Khan *et al.* 2013[16] and Bais *et al.* (2017)[45] who found that rivastigmine enhanced the memory of rats treated with $AlCl_3$. Rivastigmine is an acetylcholinesterase inhibitor (AChE-I). Inhibition of Ach-E enzyme increases acetylcholine (A-Ch) in the synapses which augments neurotransmission[1]. It is worth mentioning that defective cholinergic transmission is one of the main factors in the etiopathogenesis of memory deficit in AD patients[45].

Rahim *et al.* (2017)[17] attributed the memory-improving effect of CO to increased cholinergic activity, elevated antioxidants, diminished oxidative stress and the presence of ketones. CO, is rich in medium-chain triglycerides (MCTs) which are metabolized to ketones that can cross the blood-brain barrier (BBB) to supply a rapid energy source to neurons.

The current work showed significant increase of Ach-E enzyme level in both serum and brain homogenates of subgroups IIa, IIb, IIc and IId as compared to control due to exposure to $AlCl_3$. Additionally, a significant increase of Ach-E activity was detected in subgroup IIb (recovery group) as compared to subgroup IIa. This was in agreement with Al-Bishri *et al.* (2017)[46]; Yin *et al.* (2020)[47] and Attia and Ahmed, (2020)[48] who illustrated that Ach-E increased in the hippocampus of the $AlCl_3$-induced cognitive impaired rats. Moreover, Mahdy *et al.* (2014)[49] detected increased level of Ach-E in rats received $AlCl_3$ (for 4 weeks) after 12 weeks without treatment.

Acetylcholine levels were reported to be decreased in AD rats as a result of its degradation by Ach-E and this contributes to inadequate signal transmission leading to AD pathology[46]. Interestingly, Aluminum was stated to be a powerful choline toxin in rats which reduces A-Ch levels at the synaptic clefts when it enters the brain[50].

The current study, showed that Ach-E enzyme activity was decreased significantly in subgroups IIc, IId and IIe as compared to subgroups IIa and IIb. No significant change was detected between subgroups IIc, IId, and IIe when compared to each other, neither between subgroup IIe (rivastigmine and CO treated group) and control group. Accordingly, the synergistic effect of CO and rivastigmine lowered the Ach-E enzyme near to normal.

Going parallel with our results are the findings of Bindhu and Vijayalakshmi, (2019)[50] who found that treatment of AD rats with rivastigmine led to significant increase in A-Ch levels as well as improved behavioral and biochemical parameters when compared with non-treated AD rats. Degeneration of cholinergic neurons in the AD brain leads to reduction in A-Ch levels, leading to cognitive deficits. The ChE-Is decrease degradation of A-Ch and enhance cholinergic transmission in AD patients[51,52].

Mirzaei *et al*. (2019)[53] reported that supplementation with CO markedly attenuated Ach-E activity in the brains of AD rats. Furthermore, Attia and Ahmed, (2020)[48] revealed that CO treatment significantly ameliorated the elevation of Ach-E in tissue and serum induced by $AlCl_3$ in rats. They hypothesized that polyphenol compounds of CO could modulate Ach-E activity and improve cholinergic neurotransmission.

The current study showed significant decrease of GSH concentration in subgroups IIa, IIb, IIc and IId as compared to control group. Additionally, a significant decrease of GSH was detected in subgroup IIb (recovery group) as compared to subgroup IIa. Similarly, Yin *et al*. (2020)[47] have previously reported that GSH was declined in cognitively impaired $AlCl_3$-induced AD rats. Also, Saba *et al*. (2017)[8] demonstrated that waiting 35 days without treatment further deteriorated the neuronal metabolic activity in $AlCl_3$ mice.

Glutathione regulates cellular functions properly against oxidative stress[47]. Bindhu and Vijayalakshmi, (2019)[50] demonstrated that $AlCl_3$ administration in rats resulted in marked oxidative stress, shown by decrease in GSH levels. They explained that this could be due to the reduced mitochondria turnover and reduction of synaptic vesicles induced by Al treatment. It must be noted that brain regions vulnerable to neurodegeneration are more prone to oxidative damage and have lowered antioxidant mechanisms[54].

A significant increase of GSH concentration was recorded in subgroups IIc, IId and IIe as compared to subgroups IIa and IIb. No significant change in subgroup IIe was detected as compared to control group. So, the synergistic effect of CO and rivastigmine raised GSH levels near to normal. In agreement with the current study, Khan *et al*. (2013)[16] found that rivastigmine enhanced the reduced GSH activity significantly as compared to $AlCl_3$ treated rats. Also, Bindhu and Vijayalakshmi, (2019)[50]

stated that treatment of AD rats with rivastigmine led to an improvement in the oxidative stress.

Rahim *et al*. (2017)[17] stated that, treatment with CO increased production of antioxidants in rat brain such as GSH. The antioxidant properties of CO could be attributed to its content of polyphenols[55]. Mirzaei *et al*. (2018)[56] stated that CO is capable of creating a suitable substrate for astrocytes for the synthesis of GSH which can improve cellular damage in the hippocampus of AD model rats.

Concerning the hippocampal histological sections from subgroup IIa (AD group), marked changes were revealed in CA1, CA3 and DG in the form of degenerated and loosely arranged pyramidal cells in SP and degenerated granular cells in UL of DG in SG, in addition to the presence of glial cells with pyknotic nuclei, wide areas of vacuolations and blood vessel dilatation in the neuropil. These changes could be attributed to the neurotoxic effect of $AlCl_3$. The pyknotic nuclei and shrunken irregular cells indicate cell degeneration and death. The vacuolation in the neuropil could be due to cell loss or due to damage of dendritic or axonal processes.

These findings were consistent with preceding studies in which $AlCl_3$-intoxicated rats showed numerous degenerating cells within the CA1 and CA3 regions[34,55,57]. Yin *et al*. (2020)[47] revealed a similar image with vacuolar spaces around the neurons in $AlCl_3$-induced AD in rats. Ghoneim *et al*. (2015)[58] and Mokhemer *et al*. (2019)[59] found congested blood capillaries, shrinkage of granular cells of DG with cell loss and vacuolation after exposure of rats to $AlCl_3$. Kumar *et al*. (2019)[60] found that CA1 and CA3 regions of $AlCl_3$ group rats showed less cell density and irregularly shaped hyper-dense cells.

Mokhemer *et al*. (2019)[59] stated that $AlCl_3$ was documented to be a potent pro-oxidant in rat's brain tissues. In addition, it caused disturbance of iron homeostasis, leading to free iron ions accumulation which consequently lead to oxidative damage that finally caused neurodegeneration.

Subgroup IIb (recovery group) sections showed nearly the same picture of subgroup IIa but with more degenerated neurons. This indicated that the effect of $AlCl_3$ toxicity lasted for 30 days after withdrawal. The previous suggestion was supported by the work of Mahdy *et al*. (2014)[49] who showed that sections of brains of rats receiving $AlCl_3$ for four weeks and left without treatment for twelve weeks exhibited necrosis confirming continuity of $AlCl_3$ impact even after its withdrawal.

In the current study, subgroups IIc, IId and IIe (subgroups treated with rivastigmine, CO and both together) showed regularly arranged intact pyramidal cells in SP of CA1 and CA3 with few degenerated cells in subgroup IIc, some in IId and sparse ones in IIe. The UL of the DG showed intact granular neurons with some degenerated cells in subgroup IIc, many in IId and few ones in IIe. Vacuolations in the neuropil were noticed. Few glial cells with pyknotic nuclei

were also detected. The picture of subgroup IIe was closely near to control group which indicates the synergistic role of CO and rivastigmine.

These findings were in agreement with Khalil *et al*. (2020)[55] who showed that the hippocampus of AD rats treated with rivastigmine appeared normal. Furthermore, Bailey *et al*. (2011)[61] demonstrated that rivastigmine can preserve neuronal morphology as well as pre-synaptic protein markers in degenerating rat neuronal culture model. Rivastigmine was found to decrease Aβ secretion, suggesting a mechanism for the neuropreservation.

The findings of Mirzaei *et al*. (2019)[53] also agreed with our picture as they showed that intact neurons increased in CA1 and CA3 with CO treatment in Aβ-induced AD in rats. Also, Attia and Ahmed, (2020)[48] illustrated that CO protected against AlCl$_3$-induced neurodegeneration in rats and preserved the normal histological architecture in the hippocampus. Anti-oxidative and cholinergic anti-inflammatory mechanisms of CO could ameliorate neuroinflammation, reduce Aβ accumulation, increase neuronal survival and prevent neurodegeneration in experimental rats[62].

Consistently, Khalil *et al*. (2020)[55] illustrated that CO exerted a protective action as that of rivastigmine in maintaining normal histological structure of the hippocampus in rats received AlCl$_3$, which demonstrates the potent protective effect of CO.

The histological examination of subgroup IIa stained with anti-GFAP antibody revealed strongly immunopositive astrocytes closely related to the degenerated neurons. Subgroup IIb revealed nearly the same picture although, the mean area % of GFAP positive immunoreaction was higher in subgroup IIb compared to subgroup IIa but with nonsignificant difference. The morphometric values showed a significant increase of the mean area % of GFAP positive immunoreactivity in subgroups IIa, IIb, IIc and IId as compared to control group. This picture could be attributed to Al neurotoxicity and neurodegeneration.

It was previously reported that Al causes extensive expression of astrocytes "astrogliosis" which was seen in neurodegenerative conditions as AD in rat model[63]. Attia and Ahmed, (2020)[48] reported that in AlCl$_3$-treated rats, prominent reactive astrocytes were revealed in GFAP immunohistochemically stained sections. Similarly, Ghoneim *et al*. (2015)[58] described an increase in the number of intensely stained GFAP immunoreactive astrocytes in the AlCl$_3$-treated rats compared to control.

Cao *et al*. (2016)[64] stated that Al accumulation leads to neuroinflammation through activation of microglia and astrocytes, which is a crucial event that occurs during AD. Reactive astrocytes help to limit the spread of inflammatory cells and surround Aβ plaques. Conversely, they cause neurotoxicity by producing reactive oxygen species (ROS) and inflammatory cytokines such as interleukins (IL-1β and IL-6). It is worth mentioning that AD patients have high levels of pro-inflammatory cytokines[65], activation of which results in reduction of Aβ clearance and phagocytosis by activated glial cells which causes elevation in Aβ load[66].

Examination of sections from subgroups IIc, IId and IIe stained with anti-GFAP antibody revealed reduced immunoreaction as compared to subgroups IIa and IIb. Morphometric values showed a significant decrease in GFAP mean area % in subgroups IIc, IId and IIe as compared to subgroups IIa and IIb. However, no significant change was detected between subgroup IIe and control group which indicated that the combined effect of rivastigmine and CO significantly decreased the astrogliosis. In agreement with the present results, Mohamed *et al*. (2016)[67] reported that treatment with rivastigmine resulted in a significant reduction in astrogliosis in AD mice. Also, they proved that rivastigmine treatment decreased IL-1β levels in brain and plasma, which was consistent with its anti-astrogliosis effect. As for CO, Morris *et al*. (2020)[68] stated that entry of ketone bodies into astrocytes stimulates mitochondrial metabolism, which is capable of reducing oxidative stress and inflammation in rat brain thus, prevents the severity of astrogliosis.

Previous studies have used Aβ1-42 immunostaining to detect amyloid plaques[69,70]. The Aβ plaques originate from the buildup and aggregation of the Aβ peptide. Aβ 42 is prone to aggregation and considered to be the most toxic species. It causes synaptic dysfunction, neuronal loss and neurotransmitter deficits which lead to cognitive and memory impairment associated with AD patients[6].

Hippocampal sections from subgroup IIa stained with anti-Aβ1-42 antibody revealed strong positive immunoreaction. Multiple strong positive amyloid plaques were observed in SR layer of CA1 and CA3, and SM layer of UL of the DG. Subgroup IIb revealed nearly the same picture with presence of Aβ plaques near blood vessels. The mean values of Aβ1-42 optical density and Aβ mean area % showed a significant increase in subgroups IIa, IIb, IIc, IId and IIe as compared to control group due to exposure to AlCl$_3$. This indicates the continuous neurotoxic effect of AlCl$_3$. Aβ plaques near blood vessels seen in subgroup IIb could be due cerebral amyloid angiopathy (CAA).

In accordance, Wei *et al*. (2017)[69] reported that the plaques containing Aβ1-42 in hippocampus were significantly increased in mice treated by AlCl^3 compared to the control group. Similarly, Al has been previously shown to directly enhance Aβ load in brain of experimental rats[6,40]. Klakotskaia *et al*. (2018)[71] found mostly diffuse and some dense Aβ plaques between CA1 pyramidal layer and the alveus, several dense plaques under CA1 pyramidal layer and more frequent and denser Aβ plaques between the granular layer of the DG and hippocampal fissure in AD rats. They added that leptomeningeal and cortical blood vessels were stained dark brown indicating CAA in which Aβ deposits in and around the blood vessel wall. They stated that it is strongly associated with AD.

Exposure to AlCl$_3$ speeds up both Aβ generation and oligomerization[72] as Al is a cross-linker that enhances the polymerization of Aβ by inducing protein misfolding and self-aggregation which is involved in AD[37].

Sections from subgroups IIc and IId stained with anti-Aβ 1-42 antibody revealed moderate positive immunoreaction. Some moderate positive immunostained amyloid plaques were observed in SR layer of CA1, few in CA3 and near blood vessels. Many immunostained amyloid plaques were seen in SM layer of UL of the DG in subgroup IIc while multiple ones were observed in subgroup IId.

These findings were parallel with the morphometric measurement which denotes a significant decrease of Aβ1-42 optical density and Aβ mean area % in subgroups IIc and IId compared to subgroups IIa and IIb. Also significant decrease in subgroup IIc was detected compared to subgroup IId. This finding indicates that rivastigmine treatment offered better results than CO in reducing the amyloid plaques.

The Aβ peptide is generated from its precursor protein (APP) by β-secretase and γ-secretase endoproteolysis. Alternative APP cleavage by α-secretase prevents the generation of toxic Aβ and produces a neuroprotective and neurotrophic secreted sAPPα fragment. Rivastigmine inhibits β-secretase mRNA levels, which increases APP processing via the α-secretase pathway, thus, rivastigmine treatment was demonstrated to direct APP processing to the non-amyloidogenic pathway in rat and human cell cultures, and postmortem human samples[73].

Agreeing also with our results, Mirzaei *et al.* (2019)[53] demonstrated that amyloid accumulation was significantly reduced by CO in the hippocampus of rats. Also, cell culture of mouse neuronal cells demonstrated that CO reduced APP expression, which decreased the Aβ secretion and protected neuronal cells against Aβ induced neurotoxicity[74]. Another explanation was provided by Fernando *et al.* (2015)[13] who stated that the hydroxyl group of phenolic compounds can bind to the hydrogen of Aβ and reduce its accumulation. Ferulic acid is a phenolic compound found in the CO which has the capability of anti-accumulation of Aβ.

Sections from subgroup IIe stained with anti-Aβ1-42 antibody revealed weak positive immunoreaction for Aβ1-42. No plaques were detected in CA1 and CA3. While, few mild positive immunostained amyloid plaques were observed in SM layer of the UL of the DG. This was proved by morphometric measurements which revealed a significant decrease of Aβ optical density and Aβ mean area % in subgroup IIe compared to subgroups IIa, IIb, also, subgroups IIc and IId. These findings indicated that combination of rivastigmine and CO gave much better results in reducing the amyloid plaques.

This goes parallel with Galvin, (2012)[75] who reported that the efficacy of medium-chain triglycerides (MCTs) for the treatment of mild-to-moderate AD have been assessed in patients subjected to cognition tests. Patients administered MCTs with standard AD drugs demonstrated significant difference from placebo.

CONCLUSION

Prophylactic administration of CO improved cognitive memory and ameliorated the neurodegeneration of the hippocampus in AD induced rats as it acted as antioxidant and anti-inflammatory. Rivastigmine as a therapeutic drug, was able to restore the integrity of the hippocampus and improved cognitive memory and gave much better results in reducing amyloid plaques as compared to CO. Administration of CO and rivastigmine together had superior effect as compared to each of them alone. CO can be considered as a promising dietary supplement for protection against AD and as a part of a complementary therapy being nontoxic, inexpensive, palatable and widely available.

CONFLICT OF INTERESTS

There are no conflicts of interest.

REFERENCES

1. Abeysinghe AADT, Deshapriya RDUS and Udawatte C: Alzheimer's disease; a review of the pathophysiological basis and therapeutic interventions in Life Sci (2020) 256: 117996-118023.

2. Terracciano A and Sutin AR: Personality and Alzheimer's disease: An integrative review in Personal Disord (2019) 10(1): 4-12.

3. Whittington RA, Planel E and Terrando N: Impaired Resolution of Inflammation in Alzheimer's Disease: A Review in Front Immunol (2017) 8: 1464-1472.

4. Moir RD, Lathe R and Tanzi RE: The antimicrobial protection hypothesis of Alzheimer's disease in Alzheimers Dement (2018) 14 (12): 1602-1614.

5. Bhattacharjee S, Zhao Y, Hill JM, Percy ME and Lukiw WJ: Aluminum and its potential contribution to Alzheimer's disease (AD) in Front Aging Neurosci (2014) 6:62-65.

6. Cao Z, Wang F, Xiu C, Zhang J and Li Y: Hypericum perforatum extract attenuates behavioral, biochemical, and neurochemical abnormalities in Aluminum chloride-induced Alzheimer's disease rats in Biomed Pharmacother (2017) 91: 931-937.

7. Justin Thenmozhi A, Dhivyabharathi M, Manivasagam T and Essa MM: Tannoid principles of Emblica officinalis attenuated aluminum chloride induced apoptosis by suppressing oxidative stress and tau pathology via Akt/GSK-3βsignaling pathway in J Ethnopharmacol (2016) 194: 20–29

8. Saba K, Rajnala N, Veeraiah P, Tiwari V, Rana RK, Lakhotia SC and Patel AB: Energetics of Excitatory and Inhibitory Neurotransmission in Aluminum Chloride Model of Alzheimer's Disease: Reversal of Behavioral and Metabolic Deficits by Rasa Sindoor in Front Mol Neurosci (2017) 10: 323-338.

9. Elmorsy E, Elsharkawy E, Alhumaydhi FA and Salama M: The protective effect of Indian Catechu methanolic extract against aluminum chloride-induced neurotoxicity, A rodent model of Alzheimer's disease in Heliyon (2021) 7(2): e06269- e06279.

10. Ferreira-Vieira TH, Guimaraes IM, Silva FR and Ribeiro FM: Alzheimer's disease: Targeting the Cholinergic System in Curr Neuropharmacol (2016)14(1): 101-115.

11. Lei E, Vacy K and Boon WC: Fatty acids and their therapeutic potential in neurological disorders in Neurochem Int (2016) 95: 75-84.

12. Nafar F, Clarke JP and Mearow KM: Coconut oil protects cortical neurons from amyloid beta toxicity by enhancing signaling of cell survival pathways in Neurochem Int (2017) 105: 64-79.

13. Fernando W M, Martins I J, Goozee K G, Brennan C S, Jayasena V, and Martins R N: The role of dietary coconut for the prevention and treatment of Alzheimer's disease: potential mechanisms of action in Br J Nutr (2015) 114(1):1-14.

14. Justin Thenmozhi A,William Raja TR, Manivasagam T, Janakiraman U and Essa MM: Hesperidin ameliorates cognitive dysfunction, oxidative stress and apoptosis against aluminium chloride induced rat model of Alzheimer's disease in Nutr Neurosci (2017) 20(6): 360–368

15. Alghamdi B S A : Possible prophylactic anti-excitotoxic and anti-oxidant effects of virgin coconut oil on aluminium chloride induced Alzheimer's in rat models in J Integr Neurosci (2018) 17(3-4): 593-607.

16. Khan KA, Kumar N, Nayak PG, Nampoothiri M, Shenoy RR, Krishnadas N, Rao CM and Mudgal J: Impact of caffeic acid on aluminium chloride-induced dementia in rats in J Pharm Pharmacol (2013) 65(12): 1745-1752

17. Rahim N S, Lima S M, Mani V, AbdulMajeed A and Ramasamya K: Enhanced memory in Wistar rats by virgin coconut oil is associated with increased antioxidative, cholinergic activities and reduced oxidative stress in Pharm Biol (2017) 55(1): 825–832.

18. Olajide OJ, Yawson EO, Gbadamosi IT, Arogundade TT, Lambe E, Obasi K, Lawal IT, Ibrahim A and Ogunrinola KY: Ascorbic acid ameliorates behavioural deficits and neuropathological alterations in rat model of Alzheimer's disease in Environ Toxicol Pharmacol (2017) 50: 200-211.

19. Hidaka N, Suemaru K, Takechi K, Li B and Araki H: Inhibitory effects of valproate on impairment of Y-maze alternation behavior induced by repeated electroconvulsive seizures and c-Fos protein levels in rat brains in Acta Med Okayama (2011) 65(4): 269–277.

20. Justin-Thenmozhi A, Dhivya Bharathi M, Kiruthika R, Manivasagam T, Borah A and Essa MM: Attenuation of Aluminum Chloride-Induced Neuroinflammation and Caspase Activation Through the AKT/GSK-3β Pathway by Hesperidin in Wistar Rats in Neurotox Res (2018) 34(3): 463-476.

21. Miao Y, He N and Zhu JJ: History and new developments of assays for cholinesterase activity and inhibition in Chem Rev (2010) 110(9):5216-5234.

22. Tipple TE and Rogers LK: Methods for the Determination of Plasma or Tissue Glutathione Levels in Methods Mol Biol (2012) 889: 315–324.

23. Khalaf AA, Moselhy WA and Abdel-Hamed MI: The protective effect of green tea extract on lead induced oxidative and DNA damage on rat brain in Neurotoxicology (2012) 33(3): 280-289.

24. Roshankhah S, Jalili C and Salahshoor MR: Protective effects of Petroselinum crispum on ischemia/reperfusion-induced acute kidney injury in rats in Physiol Pharmacol (2019) 23(2): 129-139.

25. Venkataraman PS, elvakumar K, Krishnamoorthy G, Muthusami S, Rameshkumar R, Prakash S and Arunakaran J: Effect of melatonin on PCB (Aroclor 1254) induced neuronal damage and changes in Cu/Zn superoxide dismutase and glutathione peroxidase-4 mRNA expression in cerebral cortex, cerebellum and hippocampus of adult rats in Neurosci Res (2010) 66(2): 189-197.

26. Gage GJ, Kipke DR and Shain W: Whole animal perfusion fixation for rodents in J Vis Exp (2012) 65: 3564-3572.

27. Kiernan J: Histological and Histochemical Methods: Theory and Practice.5th ed., Scoin publisher, United Kingdom. (2015) pp: 111-162.

28. Suvarna k, Layton C and Bancroft J: Immunohistochemical techniques & transmission electron microscopy in Bancroft's Theory & Practice of Histological techniques, 7th ed, Elsevier health sciences, China. (2012) pp: 381-426.

29. Emsley R, Dunn G and White IR: Mediation and moderation of treatment effects in randomized controlled trials of complex interventions in Stat Methods Med Res (2010) 19(3): 237-270.

30. Martín-Belmonte A, Aguado C, Alfaro-Ruíz R, Moreno-Martínez AE, de la Ossa L, Martínez-Hernández J, Buisson A, Früh S, Bettler B, Shigemoto R, Fukazawa Y and Luján R: Reduction in the neuronal surface of post and presynaptic GABAB receptors in the hippocampus in a mouse model of Alzheimer's disease in Brain Pathol (2020) 30(3): 554-575.

31. Ułamek-Kozioł M, Czuczwar SJ, Kocki J, Januszewski S, Bogucki J, Bogucka-Kocka A and Pluta R J: Dysregulation of Autophagy, Mitophagy, and Apoptosis Genes in the CA3 Region of the Hippocampus in the Ischemic Model of Alzheimer's Disease in the Rat in J Alzheimers Dis (2019) 72(4):1279-1286.

32. Dudek SM, Alexander GM and Farris S: Rediscovering area CA2: unique properties and functions in Nat Rev Neurosci (2016) 17(2): 89-102.

33. Pomilio C, Pavia P, Gorojod RM, Vinuesa A, Alaimo A, Galvan V, Kotler ML, Beauquis J and Saravia F: Glial alterations from early to late stages in a model of Alzheimer's disease: Evidence of autophagy involvement in Aβ internalization in Hippocampus (2016) 26(2):194-210.

34. Falode JA, Akinmoladun AC, Olaleye MT and Akindahunsi AA: Sausage tree (Kigelia africana) flavonoid extract is neuroprotective in AlCl 3-induced experimental Alzheimer's disease in Pathophysiology (2017) 24(4): 251-259.

35. Zhao Y, Dang M, Zhang W, Lei Y, Ramesh T, Veeraraghavan VP and Hou X: Neuroprotective effects of Syringic acid against aluminium chloride induced oxidative stress mediated neuroinflammation in rat model of Alzheimer's disease in J Funct Foods (2020) 71: 104009-104016.

36. Singh NA, Bhardwaj V, Ravi C, Ramesh N, Mandal AKA and Khan ZA: EGCG nanoparticles attenuate aluminum chloride induced neurobehavioral Deficits, Beta Amyloid and Tau Pathology in a Rat Model of Alzheimer's Disease in Front Aging Neurosci (2018) 10: 244-256.

37. Chavali VD, Agarwal M, Vyas VK and Saxena B: Neuroprotective Effects of Ethyl Pyruvate against Aluminum Chloride-Induced Alzheimer's Disease in Rats via Inhibiting Toll-Like Receptor 4 in J Mol Neurosci (2020) 70(6): 836-850.

38. Yang X, Du W, Zhang Y, Wang H and He M: Neuroprotective Effects of Higenamine Against the Alzheimer's Disease Via Amelioration of Cognitive Impairment, A β Burden, Apoptosis and Regulation of Akt/GSK3β Signaling Pathway in Dose Response (2020) 18(4):1559325820972205.

39. Ali AA, Ahmed HI, Elfotuh KA: Modeling stages mimic alzheimer's disease induced by different doses of aluminum in rats: focus on progression of the disease in response to time in J Alzheimers Parkinsonism Dementia (2016) 1:1–11.

40. Justin Thenmozhi A, Raja TR, Janakiraman U and Manivasagam T: Neuroprotective effect of hesperidin on aluminium chloride induced Alzheimer's disease in Wistar rats in Neurochem Res (2015) 40(4): 767-776.

41. Upadhyaya S, Gangachannaiah S and Chandrashekar P L: Effect of Piper betel leaf extract on learning and memory in Aluminium chloride induced Alzheimer's disease in Wistar rats in Biomed pharmacol J (2019) 12(3): 1425-1431.

42. Olanrewaju JA, Akinola OB, Olatunji SY, Owolabi JO, Fabiyi OS, Ukonne UE and Desalu ABO: Effects of Virgin Coconut Oil on Aluminium Chloride-Induced Alzheimer-Like Dementia in the Prefrontal Cortex in JAMPS (2018) 18(1): 1-12.

43. Oboh G, Adebayo AA, Ademosun AO and Olowokere OG: Rutin restores neurobehavioral deficits via alterations in cadmium bioavailability in the brain of rats exposed to cadmium in Neurotoxicology (2020) 77:12-19.

44. Alawdi SH, El-Denshary ES, Safar MM, Eidi H, David MO and Abdel-Wahhab MA: Neuroprotective Effect of Nanodiamond in Alzheimer's Disease Rat Model: a Pivotal Role for Modulating NF-κB and STAT3 Signaling in Mol Neurobiol (2017) 54(3): 1906-1918.

45. Bais S, Kumari R and Prashar Y: Therapeutic effect of Sinapic acid in aluminium chloride induced dementia of Alzheimer's type in rats in J Acute Dis (2017) 6(4): 154-162.

46. Al-Bishri WM, Hamza AH and Farran SK: Resveratrol Treatment Attenuates Amyloid Beta, Tau Protein and Markers of Oxidative Stress, and Inflammation in Alzheimer's disease Rat Model in Int. J. Pharm. Res. Allied Sci (2017) 6(3): 71-78.

47. Yin S, Ran Q, Yang J, Zhao Y and Li C: Nootropic effect of neferine on aluminium chloride-induced Alzheimer's disease in experimental models in J Biochem Mol Toxicol (2020) 34(2): e22429- e22436.

48. Attia HN and Ahmed KA: Protective role of functional food in cognitive deficit in young and senile rats in Behav Pharmacol (2020) 31(1):81-96.

49. Mahdy KA, Gouda NAM, Marrie AH, Yassin NAZ, El-Shenawy SMA, Farrag AH and Ibrahim BMM: Protective effect of ginger (Zingiber officinale) on Alzheimer's disease induced in rats in J Neuroinfect Dis (2014) 5(2): 159-169.

50. Bindhu KH and Vijayalakshmi A: Neuroprotective effect of Carica papaya leaf extract against aluminium toxicity: An experimental study on cognitive dysfunction and biochemical alterations in rats in Indian J Pharm Educ Res (2019) 53(3): S392-S398.

51. Kandiah N, Pai MC, Senanarong V, Looi I, Ampil E, Park KW, Karanam AK and Christopher S: Rivastigmine: the advantages of dual inhibition of acetylcholinesterase and butyrylcholinesterase and its role in subcortical vascular dementia and Parkinson's disease dementia in Clin Interv Aging (2017) 12: 697-707.

52. Li DD, Zhang YH, Zhang W and Zhao P: Meta-Analysis of Randomized Controlled Trials on the Efficacy and Safety of Donepezil, Galantamine, Rivastigmine, and Memantine for the Treatment of Alzheimer's Disease in Front Neurosci (2019) 13: 472-489.

53. Mirzaei F, Khazaei M, Komaki A, Amiri I and Jalili C: Multitarget Effects of Coconut Oil (Virgin Type) on Aβ-Induced Alzheimer's Disease Animal Model in Arch Neurosci (2019) 6(2): e85715-e85723.

54. Venkateshappa C, Harish G, Mahadevan A, Srinivas Bharath MM and Shankar SK: Elevated oxidative stress and decreased antioxidant function in the human hippocampus and frontal cortex with increasing age: implications for neurodegeneration in Alzheimer's disease in Neurochem Res (2012) 37(8): 1601-1614.

55. Khalil H, Salama H, Al-Mokaddem A, Aljuaydi S and Edris A: Edible dairy formula fortified with coconut oil for neuroprotection against aluminium chloride-induced Alzheimer's disease in rats in J Funct Foods (2020) 75(4):104296-104309.

56. Mirzaei F, Khazaei M, Komaki A, Amiri I and Jalili C: Virgin coconut oil (VCO) by normalizing NLRP3 inflammasome showed potential neuroprotective effects in Amyloid-β induced toxicity and high-fat diet fed rat in Food Chem Toxicol (2018) 118: 68-83.

57. Abd El-Rady NM, Ahmed A, Abdel-Rady MM and Ismail OI: Glucagon-like peptide-1 analog improves neuronal and behavioral impairment and promotes neuroprotection in a rat model of aluminum-induced dementia in Physiol Rep (2021) 8(24): e14651-e14663.

58. Ghoneim FM, Khalaf HA, Elsamanoudy AZ, Abo El-Khair SM, Helaly AM, Mahmoud el-HM and Elshafey SH: Protective effect of chronic caffeine intake on gene expression of brain derived neurotrophic factor signaling and the immunoreactivity of glial fibrillary acidic protein and Ki-67 in Alzheimer's disease in Int J Clin Exp Pathol (2015) 8(7): 7710-7728.

59. Mokhemer SA, Saber EA, El-Tahawy NFG, Rifaai RA and Abd El-Aleem SA: Histological changes in the hippocampus of adult male albino rats following aluminum chloride administration: evidence of aluminum induced neurotoxicity in MJMR (2019) 30(4): 155-157.

60. Kumar P, Bairy KL, Nayak V, Kumar S, Kiran A and Ballal A: Amelioration of Aluminium Chloride (AlCl^3) Induced Neurotoxicity by Combination of Rivastigmine and Memantine with Artesunate in Albino Wistar Rats in Biomed pharmacol J (2019) 12(2): 703-711.

61. Bailey JA, Ray B, Greig NH and Lahiri DK: Rivastigmine lowers Aβ and increases sAPPα levels, which parallel elevated synaptic markers and metabolic activity in degenerating primary rat neurons in PLoS One (2011) 6(7): e21954-e21965.

62. Rahim NS, Lima SM, Mani V, Hazalin N, Majeed ABA and Ramasamy K: Virgin Coconut Oil-Induced Neuroprotection in Lipopolysaccharide-Challenged Rats is Mediated, in Part, Through Cholinergic, Anti-Oxidative and Anti-Inflammatory Pathways in J Diet Suppl (2020) 18(2): 1830223-1830249.

63. Elizabeth MA, Samson P and Itohan OR: Histomorphological evaluations on the frontal cortex extrapyramidal cell layer following administration of N-Acetyl cysteine in aluminum induced neurodegeneration rat model in Metab Brain Dis (2020) 35(5): 829-839.

64. Cao Z, Yang X, Zhang H, Wang H, Huang W, Xu F, Zhuang C, Wang X and Li Y: Aluminum chloride induces neuroinflammation, loss of neuronal dendritic spine and cognition impairment in developing rat in Chemosphere (2016) 151: 289-295.

65. Frost GR and Li YM: The role of astrocytes in amyloid production and Alzheimer's disease in Open Biol (2017) 7(12): 170228-170241.

66. Kaur D, Sharma V and Deshmukh R: Activation of microglia and astrocytes: a roadway to neuroinflammation and Alzheimer's disease in Inflammopharmacology (2019) 27(4):663-677.

67. Mohamed LA, Keller JN and Kaddoumi A: Role of P-glycoprotein in mediating rivastigmine effect on amyloid-β brain load and related pathology in Alzheimer's disease mouse model in Biochim Biophys Acta (2016) 1862(4): 778-787.

68. Morris G, Maes M, Berk M, Carvalho AF and Puri BK: Nutritional ketosis as an intervention to relieve astrogliosis: Possible therapeutic applications in the treatment of neurodegenerative and neuroprogressive disorders in Eur Psychiatry (2020) 63(1): e8-e28.

69. Wei Y, Liu D, Zheng Y, Li H, Hao C and Ouyang W: Protective effects of kinetin against aluminum chloride and D-galactose induced cognitive impairment and oxidative damage in mouse in Brain Res Bull (2017) 134: 262-272.

70. Kantarci A, Aytan N, Palaska I, Stephens D, Crabtree L, Benincasa C, Jenkins BG, Carreras I and Dedeoglu A: Combined administration of resolvin E1 and lipoxin A4 resolves inflammation in a murine model of Alzheimer's disease in Exp Neurol (2018) 300: 111-120.

71. Klakotskaia D, Agca C, Richardson RA, Stopa EG, Schachtman TR and Agca Y: Memory deficiency, cerebral amyloid angiopathy, and amyloid-β plaques in APP+PS1 double transgenic rat model of Alzheimer's disease in PLoS One (2018) 13(4): e0195469-e0195484.

72. Khalifa M, Safar MM, Abdelsalam RM and Zaki HF: Telmisartan Protects Against Aluminum-Induced Alzheimer-like Pathological Changes in Rats in Neurotox Res (2020) 37(2): 275-285.

73. Ray B, Maloney B, Sambamurti K, Karnati HK, Nelson PT, Greig NH and Lahiri DK: Rivastigmine modifies the α-secretase pathway and potentially early Alzheimer's disease in Transl Psychiatry (2020) 10(1): 47-63.

74. Bansal A, Kirschner M, Zu L, Cai D and Zhang: Coconut oil decreases expression of amyloid precursor protein (APP) and secretion of amyloid peptides through inhibition of ADP-ribosylation factor 1 (ARF1) in Brain Res (2019) 1704:78-84.

75. Galvin J E: Optimizing diagnosis and management in mild-to-moderate Alzheimer's disease in Neurodegener Dis Mana (2012) 2(3): 291-304.

الملخص العربى

دراسة هستولوجيه على تأثير الريفاستجمين و زيت جوز الهند على مرض الزهايمر المستحدث تجريبيا في حصين ذكور الجرذان البيضاء البالغة

زينب محمد كامل إسماعيل، مارى عطية مرقص، منة الله محمد رجائى، سارة محمد الغندور

قسم علم الأنسجة، كلية الطب، جامعة القاهرة، القاهرة، مصر

الخلفية والهدف: مرض الزهايمر هو اضطراب تنكسي عصبي يمثل الشكل الأكثر شيوعًا للخرف. يعد الحصين من أوائل المناطق التي تتأثر بمرض الزهايمر. حاليًا ، لا يوجد علاج تام لمرض الزهايمر. تم تخطيط هذه الدراسة لتقييم تأثيرالريفاستجمين وزيت جوز الهند معًا أو بمفردهما على نموذج مرض الزهايمر المستحدث تجريبيا عن طريق كلوريد الألومنيوم في حصين ذكور الجرذان البيضاء البالغة.

المواد والطرق: تم تقسيم ٣٣ من الجرذان إلى المجموعة الأولى (المجموعة الضابطة) والمجموعة الثانية (المجموعة التجريبية المقسمة إلى المجموعات الفرعية ٢أ،٢ب،٢ج،٢د،٢هـ). تم استحداث مرض الزهايمر فى المجموعة الثانية بواسطة كلوريد الألمنيوم لمدة ٤٥ يومًا. تمت التضحية بجرذان المجموعة الفرعية ٢أ فى اليوم ٤٥، تركت المجموعة ٢ب بدون علاج لمدة ٣٠ يومًا، بينما تلقت المجموعة ٢ج ريفاستيجمين لمدة ٣٠ يومًا. تم إعطاء المجموعة ٢د كلوريد الألمنيوم في وقت واحد مع إعطاء زيت جوزالهند ثم استمر العلاج بزيت جوزالهند لمدة ٣٠ يومًا. تم إعطاء المجموعة ٢هـ كلوريد الألمنيوم في وقت واحد مع إعطاء زيت جوزالهند ثم استمر العلاج بزيت جوزالهند بالتزامن مع الريفاستجمين لمدة ٣٠ يومًا. تم إجراء اختبار تقييم الذاكرة (اختبار المتاهة-Y) وقياس مستوى أسيتيل كولين استريز فى الدم. تم قياس أسيتيل كولين استريز والجلوتاثيون فى انسجة المخ بعد التضحية. تم تحضير مقاطع المخ عند مستوى الحصين وصبغها بالهيماتوكسلين والإيوسين والصبغة النسيجية الكيميائية المناعية ضد حمض البروتين الدبقي الليفي وأميلويد بيتا ١-٤٢.

النتائج: تناقصت التغيرات التنكسية العصبية فى المجموعتين ٢ج و٢د بينما أظهرت المجموعة ٢هـ الصورة النسيجية الأكثر تحسنًا. انخفض متوسط المساحة المئوية لحمض البروتين الدبقي الليفي و متوسط الكثافة البصرية والمساحة المئوية لأميلويد بيتا ١-٤٢ فى المجموعتين ٢ج و٢د بينما تم تسجيل أقل القيم فى المجموعة ٢هـ. تحسنت نتائج أسيتيل كولين استريز والجلوتاثيون واختبار الذاكرة فى المجموعتين ٢ج و٢د بينما لوحظ التحسن الأكثر فى المجموعة ٢هـ.

الإستنتاج: كان لزيت جوزالهند أثر وقائى ضد مرض الزهايمر. أظهر الجمع بين الريفاستجمين وزيت جوزالهند تأثيرا تآزريًا كبيرًا مقارنة بالريفاستجمين أو زيت جوزالهند بمفردهما.